Journal of Materials Chemistry B

ROYAL SOCIETY OF CHEMISTRY

PAPER

View Article Online
View Journal

Cite this: DOI: 10.1039/d5tb02632f

Tailored surface functionalization of AlN nanotubes for 5-fluorouracil adsorption and encapsulation: a first-principles and molecular dynamics study

V. Abinaya, K. Janani Sivasankar, J. Sneha, K. S. Bharath Shirpi Thasan, K. Iyakutti and D. John Thiruvadigal *

The rational design of biocompatible nanocarriers is essential for improving the efficacy and safety of anticancer therapeutics. Aluminum nitride nanotubes (AlNNTs) functionalized with biologically relevant sorbic acid (SA), butyric acid (BA), amine ($-NH_2$), and carbonyl (C═O) groups are evaluated as potential delivery platforms for 5-fluorouracil (5-FU). Surface modification with these functional groups enhances the polarity, active-site reactivity, and aqueous dispersibility of AlNNTs, generating a chemically enriched interface for strong drug anchoring. Structural analysis reveals pronounced local rehybridization, increased dipole moments, and improved solvation tendencies upon functionalization. The modified systems exhibit stronger adsorption energies and enhanced charge redistribution, confirming favourable interactions and encapsulation behaviour toward 5-FU. Furthermore, the calculated activation energy barriers indicate stable drug retention under physiological conditions with the possibility of stimulus-responsive release at the therapeutic site. Collectively, these findings position dual-functionalized AlNNTs as promising and tunable nanocarriers, laying a predictive foundation for the rational design of one-dimensional platforms for precision-targeted anticancer drug delivery.

Received 26th November 2025,
Accepted 11th March 2026

DOI: 10.1039/d5tb02632f

rsc.li/materials-b

1. Introduction

The precise and efficient delivery of therapeutic agents remains a central challenge in modern medicine, particularly in oncology, where the therapeutic window of chemotherapeutic drugs is often narrow. Conventional drug delivery strategies are frequently constrained by poor solubility, low stability, non-specific biodistribution, rapid clearance, and high systemic toxicity, collectively limiting therapeutic efficacy and compromising patient outcomes.[1] This limitation is exemplified by 5-fluorouracil (5-FU), a widely employed chemotherapeutic agent for colorectal, breast, and gastrointestinal cancers. 5-FU exerts its effect by inhibiting thymidylate synthase, disrupting DNA synthesis in rapidly proliferating cancer cells.[2] Despite its clinical relevance, 5-FU is plagued by low bioavailability, rapid metabolism, and systemic toxicity,[3] highlighting the need for advanced nanocarrier systems capable of enhancing solubility, protecting against premature degradation, and achieving controlled, site-specific delivery.[4]

Nanocarrier-based systems have emerged as transformative tools to address these challenges. By providing high drug-loading capacity, protection against premature degradation, controlled or stimuli-responsive release, and surface modification for active targeting, nanocarriers enable precise delivery of therapeutic agents while minimizing off-target effects. Nevertheless, current nanocarrier platforms face persistent challenges, including limited biocompatibility, instability under physiological conditions, low targeting specificity, and suboptimal drug-loading efficiency.[5] Organic carriers, although generally biocompatible, often exhibit weak drug-binding interactions and insufficient structural robustness, whereas inorganic nanoparticles offer mechanical and chemical stability but may display cytotoxicity or limited biodegradability.[6] These limitations highlight the importance of developing tunable, biocompatible, and structurally stable nanocarriers capable of balancing drug-binding affinity, solubility, and safe degradation, motivating the exploration of one-dimensional (1D) nanomaterials with reactive surfaces and controllable functionalization for precision-targeted therapy.[7]

Among emerging 1D nanomaterials, aluminum nitride nanotubes (AlNNTs) are uniquely positioned as promising candidates for biomedical applications.[8] Structurally analogous to carbon and boron nitride nanotubes, AlNNTs demonstrate

Computational Material Science and Nanodevices Simulation Laboratory, Department of Physics and Nanotechnology, SRM Institute of Science and Technology, Kattankulathur, 603 203, India. E-mail: johnd@srmist.edu.in

exceptional mechanical strength, thermal stability, and chemical inertness, enabling them to operate under physiologically and environmentally challenging conditions.[9] Electronically, AlNNTs possess a wide and tunable bandgap (3–6 eV, depending on chirality and diameter), supporting stable semiconducting behavior, minimal electron leakage, and efficient charge-transfer capabilities.[10] The polar Al–N bonds generate localized charge distributions at aluminum and nitrogen sites, creating reactive centers for adsorption and covalent functionalization.[11] This intrinsic surface polarity allows precise anchoring of functional groups such as organic acids, amines, and carbonyl moieties, effectively modulating the surface chemistry to improve drug-binding affinity, solubility, and release kinetics. Despite these compelling features, the biomedical applications of AlNNTs remain largely unexplored, with prior studies predominantly focused on their electronic, thermal, or optoelectronic properties.[12]

Compared to widely studied nanocarriers such as carbon nanotubes (CNTs), boron nitride nanotubes (BNNTs), and Al_2O_3-based nanostructures, aluminum nitride nanotubes (AlNNTs) exhibit several distinct advantages that justify their consideration as alternative drug delivery platforms. Unlike CNTs, which often suffer from hydrophobicity, aggregation, and potential cytotoxicity unless extensively functionalized, AlNNTs possess intrinsically higher polarity and partial ionic character, leading to improved interaction with polar drug molecules and enhanced dispersion in aqueous environments. While BNNTs offer excellent chemical stability and biocompatibility, their wide band gap and chemically inert surface often limit strong drug binding and require functionalization to achieve effective loading.[13] In contrast, AlNNTs exhibit intermediate polarity and tunable electronic properties, enabling balanced drug adsorption strength that is favorable for both stable loading and controlled release.[8,14] Compared to Al_2O_3 nanostructures, which are generally zero- or two-dimensional and dominated primarily by surface adsorption,[15] the one-dimensional hollow structure of AlNNTs provides distinct advantages, including a higher surface-to-volume ratio, potential encapsulation pathways, curvature-induced charge redistribution, and enhanced tunability to surface functionalization, thereby enabling improved drug–carrier interactions and greater flexibility in tuning drug affinity and controlled release behavior.[16] These features collectively distinguish AlNNTs as a promising and complementary nanocarrier system rather than a replacement for existing platforms.

Recent experimental investigations have reported successful drug loading, pH-responsive release behavior, enhanced cytotoxicity toward cancer cells, and minimal toxicity toward normal cell lines in *in vitro* studies, thereby supporting the suitability of AlN nanoparticles for biomedical applications.[17] Additional reports discussing the application of AlN nanostructures in drug delivery further emphasize their favorable physicochemical characteristics and interaction behavior relevant to therapeutic use.[18] Moreover, the experimental synthesis and structural stability of hexagonal AlN nanotubes have been previously demonstrated[19], confirming the feasibility of AlN-based nanotubular structures.

Although direct experimental investigations on the encapsulation of 5-fluorouracil (5-FU) within aluminum nitride nanotubes (AlNNTs) remain limited, the feasibility of the proposed drug-loaded system can be reasonably justified based on experimental evidence reported for analogous nanotube-based nanocarriers. Carbon nanotubes (CNTs), which exhibit structural characteristics comparable to AlNNTs, including a hollow cylindrical geometry, high aspect ratio, and nanoscale confinement capability, have been extensively explored as drug delivery platforms. Experimental studies have demonstrated that 5-FU can be successfully loaded onto functionalized multi-walled carbon nanotubes (MWCNTs), showing high drug-loading efficiency, stable drug–carrier interactions, and controlled release behavior.[20] Notably, these systems exhibit pH-responsive drug release, with enhanced release under acidic conditions characteristic of the tumor microenvironment.[21] *In vitro* biological evaluations further confirmed that 5-FU-loaded CNTs retain or enhance anticancer efficacy relative to the free drug.[22] Given the comparable tubular morphology, internal cavity structure, and physicochemical characteristics of AlNNTs, similar host–guest interactions and encapsulation behavior are therefore anticipated.

Surface functionalization is pivotal for transforming AlNNTs into highly effective drug nanocarriers.[23] Pristine AlNNTs, although structurally stable and electronically versatile, possess relatively inert surfaces that limit interactions with polar or bioactive molecules.[24] Incorporating functional groups such as carboxyl (–COOH), amine ($-NH_2$), and carbonyl (C═O) enhances hydrophilicity, polarity, and hydrogen-bonding potential, promoting stronger drug adsorption and controlled release.[25] In this study, sorbic acid and butyric acid were selected as primary organic anchors due to their biocompatibility and inherent bioactivity. Sorbic acid, with its conjugated double bonds, facilitates π-electron delocalization, enhancing charge transfer and stabilizing adsorbed species.[26] Butyric acid, a short-chain fatty acid, improves hydrophilicity and exhibits potential anticancer activity *via* modulation of cellular metabolic pathways.[27] Complementary incorporation of amine and carbonyl groups on the opposite surface of the nanotube provides a rational strategy to fine-tune polarity, steric hindrance, and hydrogen-bonding interactions, optimizing the drug–nanotube interface for both adsorption and encapsulation of 5-FU.[28]

Previous DFT studies on carbon and boron nitride nanotubes have demonstrated that surface functionalization can substantially enhance affinity toward therapeutic agents such as 5-FU, hydroxyurea, and doxorubicin.[29–32] To ensure a physically meaningful description of functionalization effects, both edge/near-end and sidewall sites were considered. Edge atoms, characterized by lower coordination and higher chemical reactivity, provide energetically favorable anchoring points with minimal lattice distortion, whereas sidewall sites represent the dominant nanotube surface relevant for adsorption and charge redistribution. Mixed-site functionalization was also

examined to better reflect realistic experimental modification conditions better. The armchair (5,5) AlNNT was selected as a representative model due to its established structural stability, semiconducting character, and widespread use in prior first-principles studies, enabling reliable comparison with the literature while maintaining computational efficiency. Despite these advances, analogous studies on functionalized AlNNTs remain limited. The work by Al-Zuhairy *et al.*[33] provides valuable molecular insight into the interaction of 5-fluorouracil with pristine AlN nanotubes, primarily focusing on adsorption energetics, charge transfer, and electronic structure modulation. Similarly, the study reported by Changyin Gan *et al.*[34] investigates drug adsorption on AlN-based systems with emphasis on electronic response and sensing-related behavior. Earlier computational investigations, including our previous study on Carmustine-loaded AlNNTs,[35] primarily focused on surface adsorption without considering asymmetric functionalization or confinement-driven stabilization.

In contrast, the present work extends beyond these studies by introducing a systematic dual-side surface functionalization strategy using biocompatible organic acids (sorbic and butyric acids) combined with donor ($-NH_2$) and acceptor (C═O) groups, an approach not previously explored for AlNNT-based drug delivery. This study establishes a correlation between the structural modification and drug–carrier behavior, including thermodynamic stability, hybridization transitions, dipole moment enhancement, ionic character modulation, and explicit solvation behavior. Importantly, unlike earlier reports largely limited to surface adsorption, we explicitly investigate and compare both adsorption and encapsulation mechanisms, supported by molecular dynamics and NEB calculations to assess kinetic stability, improved drug-loading capacity, and controlled release feasibility.

While individual quantities such as adsorption energies or electronic properties can indeed be obtained from first-principles calculations, the novelty of the present work lies in the integration of density functional theory with molecular dynamics (MD) and nudged elastic band (NEB) analyses to resolve both dynamic stability and release kinetics, which cannot be inferred from static calculations alone. MD simulations provide insight into the temporal stability of drug–nanocarrier complexes under physiologically relevant conditions, revealing distinct fluctuation behaviors associated with surface adsorption and encapsulation. More importantly, NEB calculations yield quantitative activation barriers governing drug release pathways, thereby explicitly distinguishing thermodynamic stability from kinetic accessibility. This combined framework enables the identification of non-obvious trade-offs between drug retention and controlled release, offering predictive and actionable design principles for tunable nanocarrier performance.

Thus, while earlier studies established the fundamental suitability of AlNNTs for drug interaction, the novelty of the present work lies in its systematic functionalization strategy, deeper mechanistic insight into polarity-controlled drug retention and release, and enhanced biological relevance.

To address this gap, the present work employs first-principles density functional theory (DFT) to provide a comprehensive understanding of the interplay between dual-side functionalization, structural stability, electronic properties, and solvation effects. Detailed calculations include formation energies, charge redistribution, adsorption energies, electronic density of states, and solvation behavior, offering a predictive framework for evaluating nanocarrier performance under physiologically relevant conditions.

The primary objective of this study is to design and evaluate functionalized (5,5) AlNNTs as efficient nanocarriers for targeted 5-FU delivery. Adsorption studies were performed at reactive aluminum and nitrogen sites, and encapsulation within the nanotube cavity was considered. Analyses of structural deformation, electronic modulation, charge redistribution, binding energetics, and solvation behavior elucidate the synergistic impact of dual-side functionalization.

The novelty of this work lies in its systematic DFT-based investigation of asymmetric dual-side functionalization of AlNNTs combined with dynamic and kinetic analyses. The findings position AlNNTs as versatile, biocompatible, and chemically tunable systems for precision-targeted anticancer therapy.

In addition to its material-design contributions, this work addresses key limitations in chemotherapeutic delivery, particularly for small molecules such as 5-fluorouracil that exhibit rapid clearance, low stability, and high systemic toxicity. The functionalized AlNNTs developed here create a tunable chemical interface capable of modulating polarity, solvation, and molecular affinity, enabling more predictable drug retention and controlled release under physiologically relevant conditions.

2. Modeling and computational methods

In this study, all simulations were carried out using first-principles calculations based on density functional theory (DFT), as implemented in QuantumATK.[36] This platform enables accurate modeling of low-dimensional systems and has been extensively validated for nanomaterial studies. To efficiently describe the electronic structure of the one-dimensional aluminum nitride nanotube (AlNNT) systems, we utilized the linear combination of atomic orbital (LCAO) approach.[37] This method allows a compact yet flexible representation of wave functions, significantly reducing computational cost without compromising accuracy, making it highly suitable for systems with extended periodicity such as nanotubes. For geometry optimization, the generalized gradient approximation (GGA) was adopted with the Perdew–Burke–Ernzerhof (PBE) exchange–correlation functional.[38] PBE is well-regarded for offering a balanced trade-off between computational speed and reliable prediction of bond lengths and angles in covalently bonded nanostructures. After achieving the equilibrium configurations, a more refined functional was

employed for the evaluation of electronic properties. The r^{2}SCAN functional, which belongs to the *meta*-generalized gradient approximation (*meta*-GGA) family, was selected due to its ability to more accurately capture subtle electronic interactions and to improve the description of localized states and band gap predictions.[39] This dual-functional approach, using GGA for structure and MGGA for electronics, ensures both efficiency and accuracy across different simulation stages. Structural relaxation was carried out under stringent criteria. The maximum force tolerance was set to 0.05 eV Å^{-1}, ensuring that the system reached a mechanically stable minimum on the potential energy surface. During relaxation, a vacuum buffer of at least 20 Å in both the x and y directions was introduced to isolate the nanotube from its periodic images, thereby eliminating spurious interactions and mimicking an effectively isolated nanostructure. Given the one-dimensional nature of the nanotubes, Brillouin zone sampling was limited to the direction along the tube axis (z-axis), using a Monkhorst–Pack grid of $1 \times 1 \times 120$ k-points. This dense grid provides sufficient resolution to capture intricate variations in the electronic band structure, especially near the Fermi level, which is essential for understanding the conductive or semiconductive nature of the hybrid systems. The electronic wavefunctions were expanded using a double-zeta polarized (DZP) basis set,[40] which incorporates polarization functions to better model anisotropic charge distributions and allows for improved treatment of both bonding and lone-pair electrons in the system. To ensure numerical accuracy, a mesh cutoff energy of 250 Rydberg was adopted. This parameter defines the real-space grid density used for solving the Poisson equation and ensures well-converged total energies and charge densities. Additionally, self-consistent field (SCF) convergence was enforced to a threshold of 1×10^{-5} eV, guaranteeing stable and reproducible electronic results throughout the calculations. This multi-tiered computational setup enables a detailed analysis of both structural and electronic properties of pristine and functionalized AlNNT systems, ensuring that the theoretical predictions are reliable and directly comparable with experimental or other computational studies.

3. Results and discussion

3.1. Morphological alterations induced by functionalization

3.1.1. Geometric structure of pristine and functionalized AlNNTs. The optimised pristine aluminum nitride nanotube (AlNNT) exhibits a well-defined hexagonal lattice with a uniform Al–N bond length of 1.81 Å and internal bond angles of 122.13°. These parameters are characteristic of sp^2 hybridisation and reflect a quasi-planar geometry that imparts high structural rigidity and symmetry to the nanotube, as reported in our previous studies (Fig. 1).[41] The following configurations were investigated: AlNNT functionalized with sorbic acid and one amine group [AlNNT(SA)(–NH$_2$)], with two amine groups [AlNNT(SA)$_2$(–NH$_2$)], and the corresponding carbonyl-functionalized systems [AlNNT-(SA)(C═O)] and [AlNNT(SA)$_2$(C═O)]. A parallel series of structures was constructed for butyric acid: [AlNNT(BA)(–NH$_2$)], [AlNNT(BA)$_2$-(–NH$_2$)], [AlNNT(BA)(C═O)], and [AlNNT(BA)$_2$(C═O)] (Fig. 2) (Fig. S1).

Upon surface modification with the selected organic acids, namely sorbic acid (SA) and butyric acid (BA), notable morphological distortions emerge. Functionalization induces localized lattice strain, leading to elongation of bond lengths and compression of bond angles near the anchoring sites.[42] Specifically, the Al–O bond length increases to 1.93 Å in AlNNT–SA and 2.09 Å in AlNNT–BA, while the bond angles decrease to 101.48° and 98.93°, respectively, relative to the pristine configuration.[43] These structural deviations indicate a departure from the intrinsic planarity of the nanotube and reflect a transition toward a more distorted, less symmetric geometry. Further modification was achieved by introducing amine (–NH$_2$) and carbonyl (C═O) groups at the distal end opposite to the organic acid attachment site to explore the synergistic effects of dual-side functionalization.

3.1.2. Influence of functional groups on local bonding characteristics. The extent of structural alteration in functionalized AlNNTs is intrinsically governed by the electronic nature and chemical identity of the attached functional groups. Amine (–NH$_2$) and carbonyl (C═O) groups exert distinct influences on the local bonding environment. In NH$_2$-functionalized systems, the Al–N bond length ranges from 1.87 Å to 1.96 Å (Table S1),

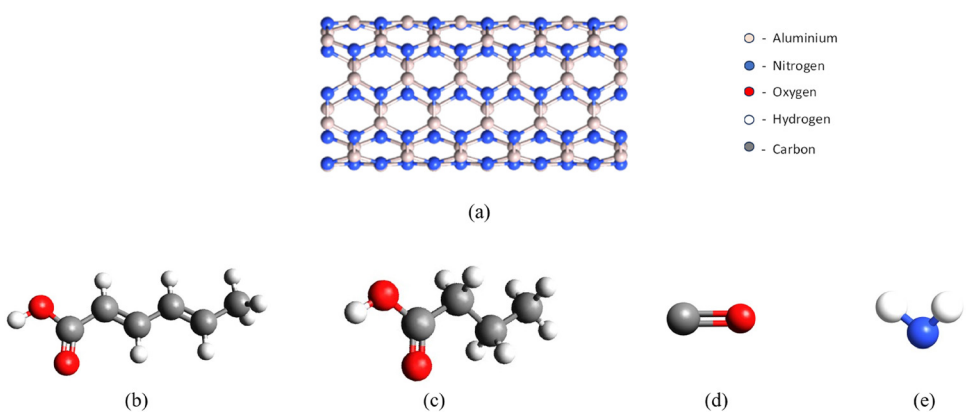

Fig. 1 Optimized geometrical structures of the modeled entities, including (a) pristine AlNNT, (b) sorbic acid, (c) butyric acid, (d) carbonyl, and (e) amine.

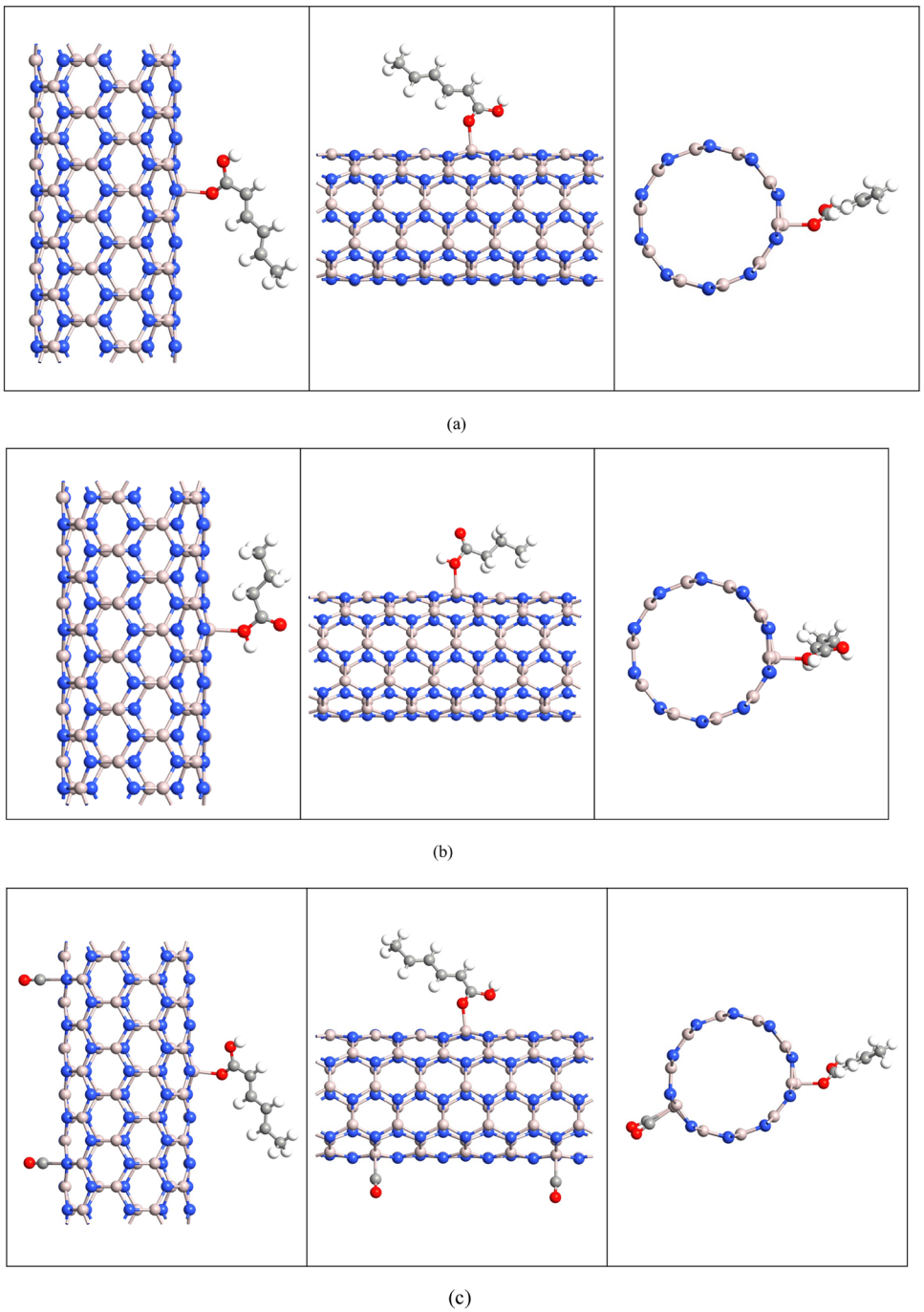

Fig. 2 Optimized side, top, and cross-sectional views of functionalized aluminum nitride nanotube systems: (a) AlNNT(SA), (b) AlNNT(BA), and (c) AlNNT(SA)2(C═O).

with only minor lattice distortion, suggesting localized perturbations at the anchoring sites.[44]

In contrast, the incorporation of carbonyl moieties induces more pronounced structural variations. In these systems, the Al–C bond length extends up to 2.10 Å, particularly in dual-site functionalized configurations, owing to charge polarization and orbital delocalization associated with the electron-withdrawing nature of the carbonyl group.[45] These changes are accompanied by a reduction in bond angles often below 99° indicating a deviation from sp^2 hybridization toward a more sp^3-like bonding character.[46]

This rehybridization is corroborated by hybridization analysis, which quantifies the redistribution of orbital character upon functionalization. The *s*-character percentage was calculated using the relation:

$$s = \frac{1}{1+m} \times 100$$

where

$$m = \frac{-1}{\cos\theta}$$

where θ represents the average bond angle of the system (Al–O, Al–C, and Al–N). The corresponding *p*-character percentage is determined as:

$$p = 100 - s$$

For the pristine AlNNT, the *s*-character is 34.71%, consistent with dominant sp^2 hybridization, as reported in our previous studies.[41] Upon functionalization, the *s*-character decreases markedly to approximately 12.70% in the highly modified systems, while the *p*-character correspondingly increases beyond 87%. This substantial shift toward higher *p*-character reflects the formation of more directional and flexible bonds.[47] Such enhanced *p*-character improves angular adaptability and polarizability of the nanostructure properties that are particularly advantageous for drug delivery.[48] Increased angular flexibility allows the functionalized AlNNT to better conform to complex biological environments, strengthening interactions with target molecules and enhancing delivery efficiency.

The variations in bond angles and the associated redistribution of *s*/*p* hybridization upon surface functionalization (Fig. 3) are indicative of localized electronic reorganization at the AlNNT surface and have direct implications for drug adsorption and stability. In particular, an increase in *p*-character reflects enhanced orbital directionality and surface polarization at the functionalized sites. Such electronic changes strengthen non-covalent interactions, including hydrogen bonding, electrostatic attraction, and dipole–dipole interactions, with polar drug molecules such as 5-fluorouracil. Even a moderate increase in *p*-character is sufficient to modify the local charge density distribution and improve the orbital overlap between surface Al/N atoms and the heteroatoms (O and N) of the drug molecule. This enhanced electronic coupling stabilizes the adsorbed or encapsulated drug configurations, contributing to stronger binding and reduced structural fluctuations at the interface. Consequently, the bond-angle distortions and hybridization changes observed upon functionalization are not merely geometric effects but are directly linked to improved drug–carrier interactions, as corroborated by the adsorption energetics and molecular dynamics stability discussed in subsequent sections.

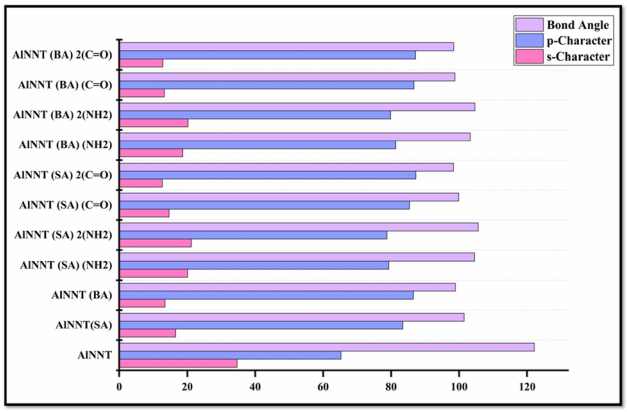

Fig. 3 Comparison between the bond angles (°) and hybridizations (*s*/*p* character) (%) of SA- and BA-functionalized AlNNT systems.

Overall, the observed variations in bond parameters underscore the chemical tunability of AlNNTs. The demonstrated ability to modulate bond lengths, bond angles, and hybridization states through strategic surface functionalization highlights the promise of AlNNT-based nanostructures as versatile platforms for targeted drug delivery and other advanced biomedical applications.

3.2. Electronic structure analysis

3.2.1. Band structure evolution and functionalization-induced modulation. The electronic band structures of the functionalized armchair (5,5) aluminum nitride nanotubes (AlNNTs) are presented in Fig. 4a–c. Functionalization with sorbic and butyric acids, together with amine ($-NH_2$) and carbonyl (–C═O) groups, induces pronounced modifications in the electronic dispersion along the Γ–Z direction. Across all systems, the energy bands near the Fermi level undergo rearrangement, reflecting strong orbital coupling between the nanotube surface atoms and the attached functional groups.

The significant difference observed between the band gaps of the SA–AlNNT (1.62 eV) and BA–AlNNT (3.73 eV), as well as the distinct variations in their band dispersions, originates from fundamental differences in the molecular electronic structures and interfacial orbital interactions introduced by sorbic and butyric acid functionalization. Sorbic acid, an unsaturated molecule containing a conjugated diene system (C═C–C═C), possesses delocalized π-electrons capable of interacting efficiently with the surface orbitals of the AlNNT. PDOS analysis of the SA–AlNNT reveals enhanced p-orbital contributions near the Fermi level arising from the sorbic acid moiety, indicating strong energetic overlap between molecular-derived π-states and the intrinsic nanotube states contributing to the valence band maximum (VBM) and conduction band minimum (CBM). This increased orbital hybridization and charge redistribution perturb the band edges, resulting in substantial band gap narrowing and modified band curvature.

In contrast, butyric acid is a saturated aliphatic molecule dominated by localized σ-bonding orbitals and lacking π-conjugation. Consequently, the PDOS of BA–AlNNT shows that molecule-induced states remain largely separated from the band edges, leading to weaker orbital coupling, reduced charge transfer, and minimal perturbation of the intrinsic AlNNT electronic structure. This preservation of the nanotube's electronic topology explains the comparatively wider band gap and less pronounced dispersion changes.

Further modulation of the electronic structure is introduced by secondary functional groups. In the amine-functionalized systems, corresponding to n-type behavior, donor states appear near the valence band maximum (VBM), bringing it closer to the Fermi level.[49] This arises from electron donation by the nitrogen lone pairs to adjacent aluminum atoms, which

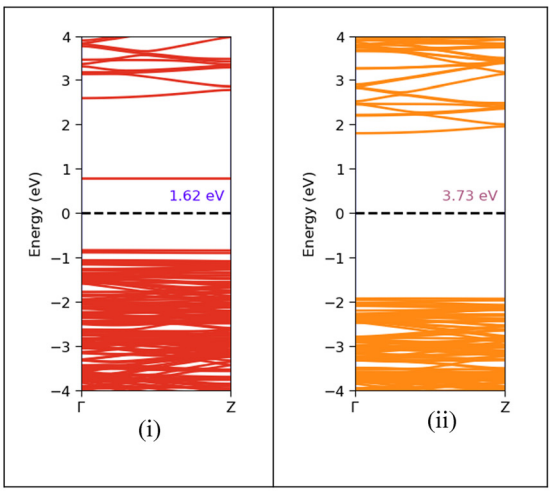

(a)

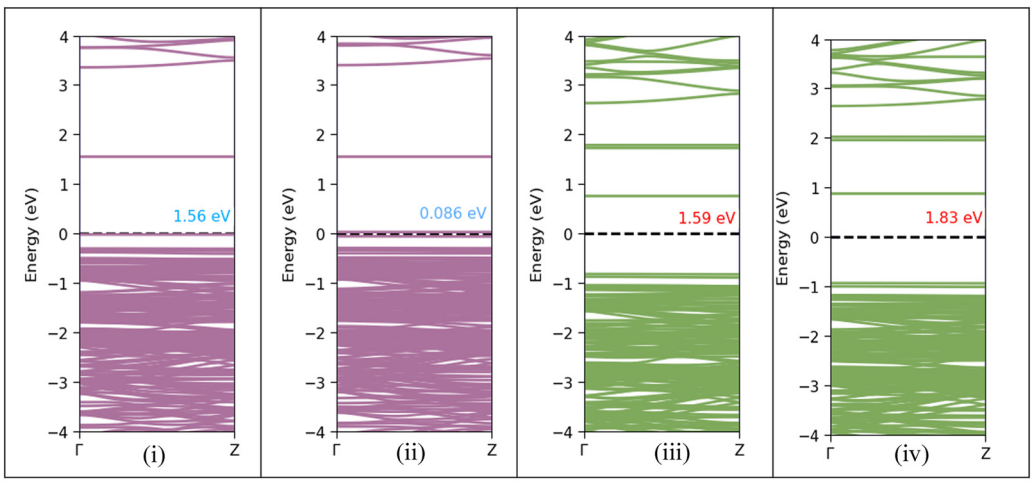

(b)

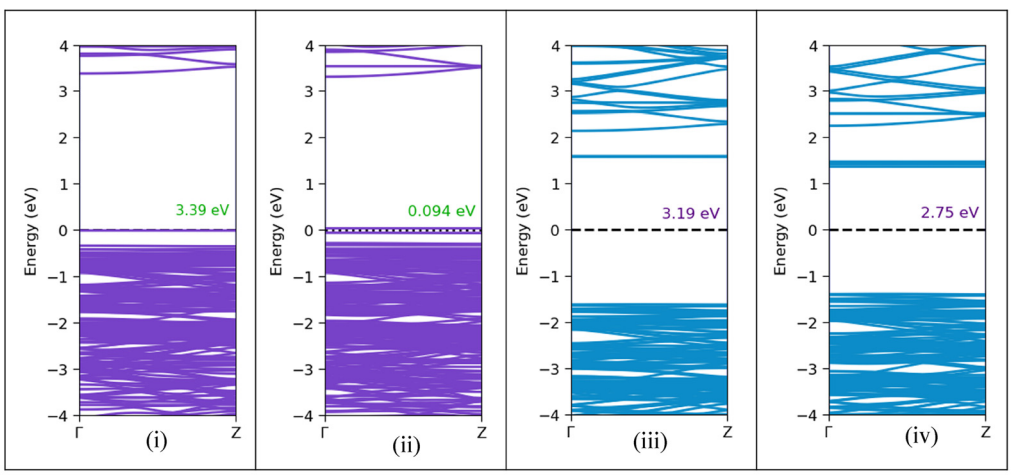

(c)

Fig. 4 (a). Band structures of the (i) AlNNT (SA) and (ii) AlNNT (BA); (b) (i) AlNNT (SA)(−NH_2), (ii) AlNNT (SA)2(−NH_2), (iii) AlNNT (SA)(C═O), and (iv) AlNNT (SA)2(C═O); (c) (i) AlNNT (BA)(−NH_2), (ii) AlNNT (BA)2(−NH_2), (iii) AlNNT (BA)(C═O), and (iv) AlNNT (BA)2(C═O).

introduces additional occupied states at the top of the valence band. Both sorbic- and butyric-acid-modified nanotubes show a narrowing of the band gap, enhanced band overlap, and partial band flattening near the Fermi level, indicating localization of electrons at the functionalization sites. The n-type modification increases the density of conduction electrons and enhances charge carrier availability, which is favorable for electron-mediated interactions during drug adsorption.[50] Conversely, the carbonyl-functionalized systems exhibit p-type behavior, characterized by the formation of acceptor states just below the conduction band minimum (CBM). The electron-withdrawing oxygen atoms pull electron density from the AlNNT surface, creating hole-like states in the valence region. In both sorbic- and butyric-acid-functionalized nanotubes, this results in a reduced band gap and the emergence of flattened conduction-edge bands, indicative of localized electronic states and strong interfacial polarization.[51] The p-type modification favors hole-mediated charge redistribution, which can influence drug binding and release processes.

Overall, these n-type and p-type modifications demonstrate that the electronic properties of AlNNTs can be systematically tuned by selecting appropriate functional groups. Donor-like amine groups inject electrons, whereas acceptor-like carbonyl groups withdraw electrons, enabling controlled modulation of orbital overlap, charge distribution, and electronic reactivity.[52] Such tunability is critical for optimizing AlNNTs as nanocarriers for charge-assisted drug adsorption and controlled release.

3.2.2. Total and projected density of states (DOS and PDOS) analysis. The total density of states (DOS) of the functionalized AlNNT (Fig. S2) and functionalized systems is shown in Fig. S3a and b. A pronounced redistribution of electronic states occurs upon surface modification, emphasizing the strong influence of chemical bonding on the nanotube's electronic structure. Across all functionalized configurations, additional states emerge near the Fermi level, accompanied by distinct shifts in the band edges. These modifications indicate that surface functionalization alters the electronic occupation and modifies the potential landscape of the nanotube framework.

Single-side functionalization introduces such discrete states near the valence- or conduction-band edges, whereas double-side functionalization (2X) enhances the spectral intensity near EF and slightly narrows the effective band gap. The DOS profiles of the 2X systems display broader features and smoother transitions between the occupied and unoccupied regions, reflecting stronger orbital coupling and partial delocalization of the induced states.[53] The emergence of these hybridized levels within or adjacent to the original gap underscores the formation of new electronic states resulting from strong chemical interactions between the nanotube surface and the attached organic fragments. For the sorbic acid (SA) based systems, characteristic flat bands are observed at the conduction-band (CB) edge. In the singly functionalized AlNNT(SA) and carbonyl-functionalized SA systems, nearly dispersionless features appear at approximately 0.9 eV above the Fermi level. In contrast, the amine-functionalized SA systems, both single and double substitutions, exhibit flat states centred around 1.6 eV at the CB edge. These flat bands correspond to localized electronic states primarily confined to the sorbic acid moiety or the attached functional groups. Owing to their spatial localization and weak hybridization with the extended AlNNT states, these levels contribute negligibly to charge transport and do not significantly alter the global band topology or the intrinsic semiconducting nature of the nanotube. Their presence merely reflects weak molecular resonances rather than defect- or impurity-induced conductive channels, thereby preserving the overall electronic integrity and stability of the system.[54]

The projected density of states (PDOS) (Fig. 5a–e) provides further insight into the orbital origin of these modifications. Decomposition of the DOS reveals that the states near E_F primarily originate from the O-2p, C-2p, and N-2p orbitals of the functional groups, which hybridize with the Al-3p and N-2p states of the nanotube surface. The extent and energetic alignment of these hybridized orbitals depend strongly on the electronegativity and bonding configuration of the substituents.

In the carbonyl-functionalized complexes, the O-2p and C-2p orbitals contribute substantial spectral weight near the upper valence region. Their strong p–p coupling with the nitrogen orbitals of the tube wall produces bonding and antibonding combinations that elevate the valence-band edge and partially populate the gap.[55] Conversely, the amine- and amide-functionalized configurations exhibit distinct N-2p features near the conduction region, corresponding to the overlap of lone-pair orbitals with unoccupied Al-3p states. These localized bonding interactions perturb the conduction-band edge and generate characteristic PDOS features near E_F.

A comparison between single- and double-side configurations reveals a consistent evolution from localized to delocalized electronic behavior. Single-side attachment yields sharp, narrow PDOS peaks that reflect localized states confined to the adsorbed moieties, while double-side functionalization broadens these peaks and merges them with the nanotube continuum, signifying enhanced orbital overlap and greater electronic dispersion along the tube axis. Such broadening indicates the emergence of spatially extended states capable of facilitating charge transport and modulating the effective conductivity of the system.[56]

The overall redistribution of DOS and PDOS originates from two coupled mechanisms: (i) orbital hybridization, which forms new bonding and antibonding combinations near the band edges and (ii) local electrostatic perturbation, induced by the polar functional groups that reshape the potential energy landscape around the adsorption sites. The appearance of weakly dispersive, flat states does not degrade the electronic performance, as these states are localized and energetically isolated from the principal conduction pathways. Collectively, these results demonstrate that controlled chemical functionalization enables fine-tuning of the electronic structure of AlNNTs

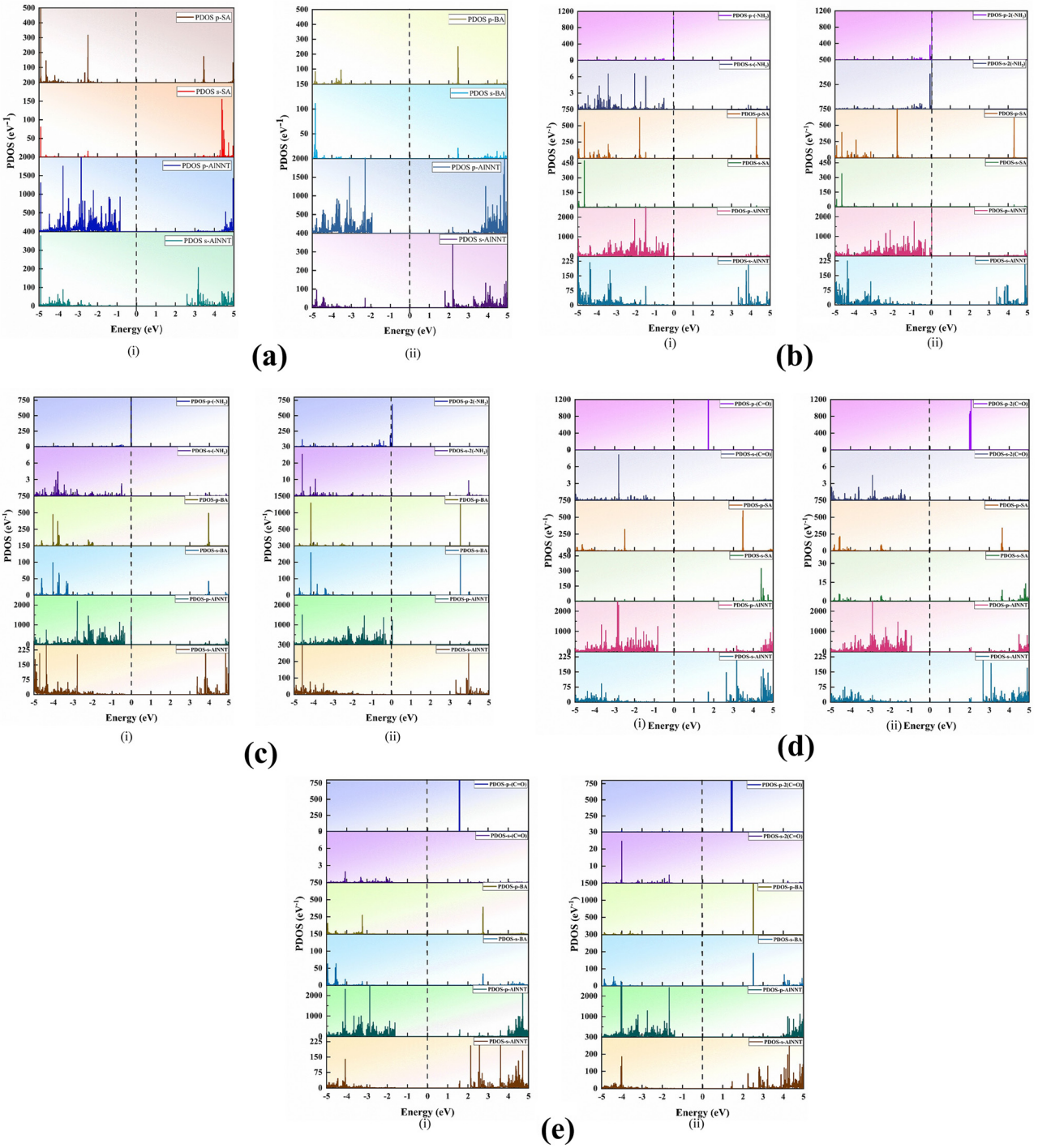

Fig. 5 (a). PDOS for (i) AlNNT (SA) and (ii) AlNNT (BA); (b) (i) AlNNT (SA)(−NH_2) and (ii) AlNNT (SA)$_2$(−NH_2); (c) (i) AlNNT (BA)(−NH_2) and (ii) AlNNT (BA)$_2$(−NH_2); (d) (i) AlNNT (SA)(C═O) and (ii) AlNNT (SA)$_2$(C═O); (e) (i) AlNNT (BA)(C═O) and (ii) AlNNT (BA)$_2$(C═O).

through targeted orbital coupling, without compromising their inherent semiconducting framework.

3.3. Thermodynamic stability assessment

3.3.1. Binding, and formation energies. The thermodynamic stability of pristine and functionalized aluminum nitride nanotubes (AlNNTs) was investigated using first-principles density functional theory (DFT), focusing on the binding energy (B.E.) and formation energy (F.E.) (Table S2). These energetic descriptors collectively provide insights into system stability, host–guest interactions, and synthetic feasibility.[57]

Binding energy quantifies the interaction strength between the AlNNT scaffold and the functional groups, providing

insight into the thermodynamic favorability of functionalization. It was calculated as:

$$\text{B.E.} = E_{\text{AlNNT–(X/2X)}} - \left(E_{\text{AlNNT}} + E_{\text{(X/2X)}}\right)$$

where $E_{\text{AlNNT–(X/2X)}}$ is the total energy of the functionalized system, E_{AlNNT} is the energy of the pristine nanotube, and $E_{\text{(X/2X)}}$ is the energy of the isolated functional molecule(s) considered in their neutral, intact form. Negative B.E. values indicate energetically favorable attachment of the functional groups.[58] In this study, AlNNT(SA)-2(NH_2) and AlNNT(BA)-2(NH_2) exhibited B.E. values of −7.25 eV and −6.78 eV, respectively, reflecting strong chemisorption due to the lone pair electrons of the amino groups donating electron density to the empty orbitals of Al or N atoms. Carbonyl-functionalized systems also showed substantial negative B.E. values, arising from π-conjugation with the AlNNT surface and dipole–dipole interactions. The trend of increasingly negative B.E. for dual-functionalized systems highlights a cooperative stabilization effect, where multiple functional groups enhance electron delocalization and interfacial interactions.

The formation energy is obtained for the AlNNT using

$$E_{\text{F.E.}} = \frac{1}{N}[E_{\text{AlN}} - X(E_{\text{Al}}) - Y(E_{\text{N}})]$$

$E_{\text{F.E.}}$ represents the formation energy, where N is the total number of atoms in the nanotube, X and Y denote the numbers of Al and N atoms, respectively, E_{AlN} is the total energy of the nanotube, and, E_{Al} and E_{N} are the reference energies of isolated Al and N atoms.

For the AlNNT (X/2X), the formation energy is obtained using equation

$$E_{\text{F.E.}} = \frac{1}{N}[E_{\text{AlNNT(X/2X)}} - X_1(E_{\text{Al}}) - X_2(E_{\text{N}}) - X_3(E_{\text{H}}) - X_4(E_{\text{C}}) - X_5(E_{\text{O}})]$$

where $E_{\text{AlNNT(X/2X)}}$ is the total energy of the functionalized nanotube, X_1–X_5 represent the numbers of Al, N, H, C, and O atoms, respectively, and $X_1(E_{\text{Al}})$, $X_2(E_{\text{N}})$, $X_3(E_{\text{H}})$, $X_4(E_{\text{C}})$ and $X_5(E_{\text{O}})$ correspond to the energies of the isolated atoms.

Formation energy indicates the thermodynamic feasibility of synthesizing the functionalized nanohybrids from their constituent components. Negative F.E. values confirm that the formation is energetically favorable and that the resulting structures are intrinsically stable.[59] All functionalized AlNNT systems in this study exhibited negative formation energies. Dual-functionalized systems, particularly those containing carbonyl (C═O) groups, demonstrated slightly more favorable F.E. values compared to amino-functionalized analogues. This enhanced stability is attributed to the π-conjugation with the AlNNT π-system and strong dipole–dipole interactions, which further lower the overall energy of the nanohybrid.

Considering the combined trends in binding, and formation energies (Fig. 6), the functionalized AlNNTs can be ranked in terms of thermodynamic stability as follows:[AlNNT(SA)$_2$(C═O)] > [AlNNT(SA)$_2$(–NH_2)] > [AlNNT(BA)$_2$(C═O)] > [AlNNT(BA)$_2$(–NH_2)] > [AlNNT(SA)(C═O)] > [AlNNT(BA)(C═O)] > [AlNNT(SA)(–NH_2)] > [AlNNT(BA)(–NH_2)] > AlNNT(SA) > AlNNT(BA). This ranking underscores that dual side functionalization with polar groups, particularly C═O, maximizes energy stabilization and binding affinity, positioning these systems as highly promising nanocarriers for targeted drug delivery applications.

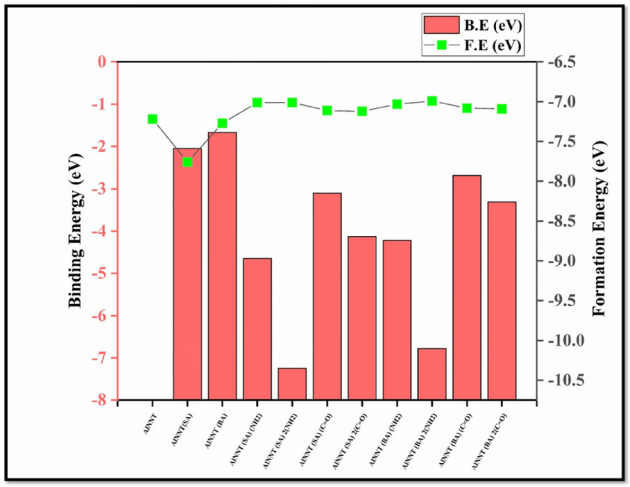

Fig. 6 Comparison of the binding energy (eV) and formation energy (eV) for the AlNNT and AlNNT-functionalized systems.

3.4. Polar character and charge redistribution

3.4.1. Mulliken charge distribution, bonding evolution, and solvation implications. The pristine aluminum nitride nanotube (AlNNT) exhibits a nearly uniform electron distribution, with Al–N Mulliken charges of –0.002*e*, indicative of highly covalent and symmetric bonding. The near-equal electron sharing between Al and N atoms results in negligible polarity, as explained in our previous study.[35]

Covalent functionalization with electron-withdrawing (–COOH and –C═O) or electron-donating (–NH_2) groups induces localized charge redistribution, quantified *via* Mulliken population analysis. Acid groups, such as sorbic acid (SA) and butyric acid (BA), withdraw electron density from adjacent Al–N bonds, generating partial positive charges on the functional moieties. Amine (–NH_2) groups act as electron donors, partially restoring electron density in the Al–N bonds. Combined donor–acceptor interactions generate pronounced polarization, with carbonyl-containing systems exhibiting the strongest charge separation. SA-functionalized systems generally show slightly higher polarization than BA analogues.

These Mulliken charge changes indicate a systematic evolution in the bonding character. The pristine AlNNT, with minimal charge differences, exhibits predominantly covalent bonding. Moderate functionalization, such as single NH_2 substitution or single acid attachment, leads to polar covalent

Table 1 Partial charge (e), dipole moment (D), ionic character (%) and solvation energy (kcal mol^{-1}) of SA- and BA-functionalized AlNNT systems

Systems	Partial charge (e)	Dipole moment (D)	Ionic character (%)	Solvation energy (kcal mol^{-1})
AlNNT(SA)	Al–N = −0.522 SA = 0.518	4.628	32.62	−32.76
AlNNT(BA)	Al–N = −0.308 BA = 0.310	3.103	19.37	−24.05
AlNNT(SA)(–NH_2)	Al–N = −0.712 (SA)(NH_2) = 0.711	6.453	44.50	−33.57
AlNNT$(SA)_2$(–NH_2)	Al–N = −0.899 $(SA)_2$(NH_2) = 0.897	8.050	56.18	−33.69
AlNNT(SA)(C═O)	Al–N = −0.978 (SA)(C═O)0.983	9.550	61.43	−34.84
AlNNT(SA)2(C═O)	Al–N = −1.448 $(SA)_2$(C═O) = 1.444	14.30	90.50	−35.42
AlNNT(BA)(–NH_2)	Al–N = −0.509 (BA)(NH_2) = 0.508	4.781	31.80	−24.82
AlNNT$(BA)_2$(–NH_2)	Al–N = −701 $(BA)_2$(NH_2) = 0.698	6.460	43.81	−25.34
AlNNT(BA)(C═O)	Al–N = −0.769 (BA)(C═O) = 0.773	7.770	48.31	−25.13
AlNNT$(BA)_2$(C═O)	Al–N = −1.234 $(BA)_2$(C═O) = 1.233	12.44	77.12	−26.01

bonds.[61] Larger charge transfers, observed in double substitutions or strong electron-withdrawing groups, produce significant ionic contributions, reflecting a transition toward partially ionic bonding. This covalent → polar covalent → partially ionic progression generates localized dipoles and enhances the overall polar character of the nanotube.

Such polarization has direct implications for solvation and dispersion. In a solvent, the induced dipoles orient surrounding molecules, enhancing interactions. Increased polarity improves water solubility and colloidal stability, which are critical for biomedical applications such as targeted drug delivery.

3.4.2. Dipole moment evolution. The bond dipole moment (μ) of the AlNNT systems was calculated using:

$$\mu = q \times d$$

where $q = e \times$ P.C. (partial charge), $e = 1.6 \times 10^{-19}$ C is the elementary charge, P.C. is the Mulliken partial charge, and d is the bond length. This approach quantifies axial charge asymmetry induced by functionalization.

Consistent with the Mulliken analysis, the pristine AlNNT shows a negligible dipole (∼0.017 D), reflecting its symmetric, nonpolar nature, explained in our previous study.[35] Functionalization with polar acids generates moderate dipoles (3–5 D) (Table 1), while the addition of electron-donating NH_2 groups further enhances polarization *via* a donor–acceptor mechanism.[60] Carbonyl-functionalized systems exhibit the largest dipoles, exceeding 12 D in double substitution cases, in agreement with the strongest charge separations.[61]

The evolution of dipole moments mirrors the changes in bond character and Mulliken charge redistribution: stronger donor–acceptor interactions and higher electron transfer yield larger dipoles, which improve solvent orientation, solubility, and dispersion stability, key factors for biomedical applicability.

3.4.3. Ionic character assessment. The percentage ionic character (PIC) was estimated based on the calculated atomic partial charges obtained from Mulliken charge population analysis.

The PIC was evaluated using

$$\mathrm{PIC} = \frac{\mathrm{P.C.}}{e} \times 100$$

where P.C. represents the magnitude of the atomic partial charge and e is the elementary charge. The partial charges were derived from the charge population analysis of the optimized structures. This approach provides a quantitative measure of the degree of charge separation and the relative ionic contribution within the Al–N framework.

The percentage ionic character provides a direct measure of the transition from purely covalent to increasingly ionic bonding within the Al–N framework. The pristine AlNNT exhibits an almost negligible ionic character (∼0.12%), reflecting its highly covalent nature and symmetric electron distribution, explained in our previous study.[41] Functionalization with polar acids significantly enhances the ionic contribution. Sorbic acid increases the ionic character to 32.62%, whereas butyric acid yields a lower value of 19.37%, consistent with its aliphatic, non-conjugated molecular structure and comparatively weaker electron-withdrawing effect.

The introduction of additional polar groups further amplifies the ionic nature. NH_2 donor groups raise the ionic character to 56.18% for [AlNNT$(SA)_2$(NH_2)] and 43.81% for [AlNNT$(BA)_2$(NH_2)]. Carbonyl-functionalized systems exhibit the strongest ionic characteristics, with [AlNNT$(SA)_2$(C═O)] reaching 90.50% and [AlNNT$(BA)_2$(C═O)] 77.12%. This trend clearly demonstrates that both the type and number of functional groups directly modulate the ionic behavior of the nanotube, with electron-withdrawing groups such as COOH and C═O being particularly effective.[62]

These observed changes in the ionic character correlate closely with Mulliken charge redistribution and the evolution of the dipole moment. As electron transfer increases at the functionalization sites, the Al–N bonds shift from covalent toward polar covalent and partially ionic character. This enhanced bond polarity generates larger bond dipoles, which collectively sum to higher overall dipole moments along the nanotube axis. Consequently, the interplay between ionic character, charge redistribution, and dipole evolution directly influences solvation, dispersion stability, and interfacial interactions, critical factors for the design of AlNNT-based nanohybrids in targeted drug delivery applications.

3.4.4. Electron difference density (EDD) analysis. Electron difference density (EDD) analysis provides a real-space visualization of the electron redistribution induced by functionalization. Regions of electron accumulation are indicated in yellow, while regions of electron depletion are shown in Fig. S4a–c. In all functionalized systems, electron accumulation is primarily localized around electronegative acceptor groups, such as –COOH and –C═O, while the adjacent Al–N bonds exhibit the corresponding electron depletion. This observation is consistent with Mulliken charge analysis, confirming directional charge transfer from the nanotube to the functional groups. Systems with dual substitutions show more extensive and intense accumulation–depletion patterns, reflecting stronger polarization fields along the nanotube axis. Nanohybrids containing both electron-donating (–NH_2) and electron-withdrawing (C═O) groups exhibit a pronounced push–pull pattern, which not only increases the local bond dipoles but also explains the higher overall dipole moments and elevated ionic character observed in these systems.[63]

Overall, the EDD maps provide direct visual evidence of the charge redistribution induced by functionalization, validating the trends observed in Mulliken charges, dipole moments, and ionic character. These results demonstrate that rational functionalization can effectively tune the polar nature of the AlNNT, enhancing its potential for solvation, dispersion, and targeted interactions in drug delivery applications.

3.4.5. Mechanistic insight: transition from non-polar to polar nanohybrids. Collectively, the Mulliken charge profiles, dipole moment evolution, ionic character trends, and EDD maps demonstrate that functionalization transforms the pristine AlNNT into a tunable polar nanostructure. The cooperative interplay of electron-withdrawing (–COOH and –C═O) and electron-donating (–NH_2) groups induces pronounced spatial charge separation, shifting the Al–N bonds from covalent toward a partially ionic character and generating a directional charge gradient along the nanotube axis. This controlled electron redistribution leads to adjustable dipole moments, enhanced solvation, and improved dispersion stability, which are crucial for effective non-covalent interactions with biomolecules and therapeutic agents. Such precise modulation of the polar character establishes a versatile framework for designing AlNNT-based nanohybrids for targeted drug delivery and other biomedical applications.

3.5. Solvation behavior and carrier solubility

The solubility of AlNNT-based nanohybrids in aqueous media is a critical factor for their effectiveness as drug delivery carriers, influencing dispersion stability, bioavailability, and interaction with biomolecules. To quantify solvent stabilization, continuum solvation calculations were performed using the conductor-like screening model (COSMO). This approach allows us to simulate the interaction of the nanotube surface with a polar solvent environment.[64]

The solvation energy was determined as the energy difference between the system in the aqueous phase and the gas phase, calculated as

$$E_{Sol} = E_{Water} - E_{Gas},$$

where E_{Water} and E_{Gas} correspond to the total energies obtained from calculations performed in the implicit water environment and vacuum (gas phase), respectively.

The pristine AlNNT exhibits relatively low solvation due to its nonpolar, symmetric surface, which limits favorable interactions with water. Functionalization with polar moieties, such as sorbic acid (SA) or butyric acid (BA), substantially enhances solvent stabilization. The incorporation of electron-donating (–NH_2) and electron-withdrawing (–C═O) groups further increases solvation by generating localized dipoles that align with solvent molecules and strengthen intermolecular interactions. The highest solvation is observed for the [AlNNT$(SA)_2$(C═O)] system, highlighting the synergistic effect of multiple polar groups along the nanotube axis.

Enhanced solubility has direct implications for drug delivery. Improved solvent interactions prevent nanotube aggregation under physiological conditions, ensuring uniform dispersion and maximizing the surface area available for drug adsorption. Polar surfaces also facilitate non-covalent interactions, including hydrogen bonding, dipole–dipole interactions, and electrostatic attractions, with therapeutic molecules, thereby increasing drug loading efficiency and stability.[65] Collectively, these features improve bioavailability, reduce off-target aggregation, and support controlled and efficient drug release, underscoring the importance of rational functionalization in designing AlNNT-based nanocarriers for targeted therapeutic applications.

3.6. Adsorption and Encapsulation of 5-FU on [AlNNT$(SA)_2$(C═O)]

The [AlNNT$(SA)_2$(C═O)] nanohybrid exhibited the highest aqueous solubility among the studied systems, identifying it as a promising candidate for drug delivery applications. To investigate its drug-loading capability, both surface-adsorbed (A) and encapsulated (E) configurations of the anticancer drug 5-fluorouracil (5-FU) were modeled. These configurations allow evaluation of distinct interaction modes, including non-covalent surface adsorption and internal encapsulation, which are critical for optimizing the loading efficiency, structural stability, and controlled release. Drug molecules were positioned at multiple sites interacting with Al and N atoms of

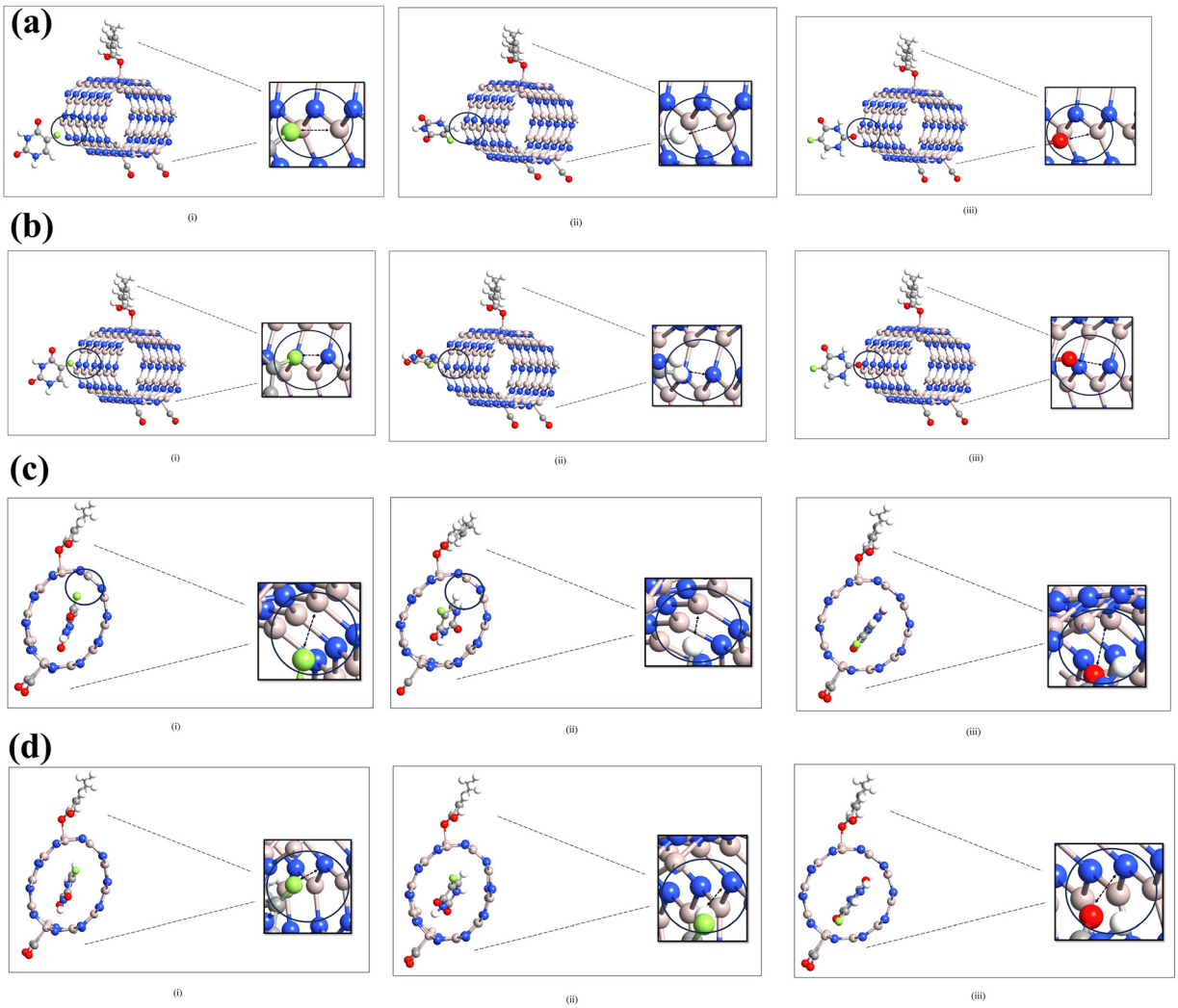

Fig. 7 (a) Adsorption of 5-fluorouracil (5-FU) at the Al site of [AlNNT(SA)$_2$(C═O)] *via* F, H, and O atom orientations. (b) Adsorption of 5-fluorouracil (5-FU) at the N site of [AlNNT(SA)$_2$(C═O)] *via* F, H, and O atom orientations. (c) Encapsulation of 5-fluorouracil (5-FU) at the Al site of [AlNNT(SA)$_2$(C═O)] *via* F, H, and O atom orientations. (d) Encapsulation of 5-fluorouracil (5-FU) at the N site of [AlNNT (SA)$_2$(C═O)] *via* F, H, and O atom orientations.

the nanotube, with the functional atoms (F, O, and H) in 5-FU facilitating adsorption and encapsulation (Fig. 7a–d).

3.6.1. Adsorption energy. For surface-adsorbed systems, adsorption energies (Table 2) ranged from −0.341 eV to −0.819 eV. The Al–F_A configuration exhibited the strongest adsorption (−0.819 eV), followed by Al–H_A (−0.756 eV) and N–H_A (−0.577 eV). Weaker adsorption was observed for Al–O_A (−0.361 eV) and N–O_A (−0.341 eV), reflecting less favorable non-covalent interactions. These results confirm the exothermic nature of physisorption, predominantly governed by van der Waals forces and weak polar contacts, making surface adsorption suitable for rapid drug loading and potential burst release.[66]

Encapsulated systems displayed substantially stronger adsorption, with energies ranging from −3.006 eV to −3.842 eV. The Al–F_E complex exhibited the most negative adsorption energy (−3.842 eV), followed by Al–H_E (−3.691 eV), N–F_E (−3.357 eV), and N–H_E (−3.346 eV). The enhanced adsorption strength arises from spatial confinement within the nanotube cavity, increased molecular surface contact, and interactions with internal polar groups, including hydrogen bonding and electrostatic stabilization.[67] These factors collectively reinforce the structural integrity of the encapsulated drug, supporting sustained release and prolonged therapeutic performance. Overall, Al–F_A (surface adsorption) and Al–F_E (encapsulation) emerged as the most favorable configurations, highlighting their potential for rapid and sustained delivery.

3.6.2. Mulliken population analysis. To complement energetic insights, Mulliken population analysis was performed to quantify the charge transfer between 5-FU and the functionalized AlNNTs, providing insight into donor–acceptor coupling, orbital hybridization, and electrostatic interactions.

In surface-adsorbed systems, charge transfer was modest ($\sim$0.15e to 0.39e), consistent with physisorption-dominated interactions. Al–F_A exhibited the highest charge redistribution ($|\Delta Q| \approx 0.388e$), followed by Al–H_A (0.380e), whereas N–F_A,

Table 2 Binding energy, Mulliken charge transfer, and the final nanotube diameter of 5-FU adsorbed (A) and encapsulated (E) on [AlNNT $(SA)_2(C{=}O)$]

Site	System	Binding energy (eV)	Partial charge (e)
Al	Al–F_A	−0.819	Carrier = −0.196, drug = 0.192
	Al–O_A	−0.361	Carrier = −0.128, drug = 0.132
	Al–H_A	−0.756	Carrier = −0.188, drug = 0.192
N	N–F_A	−0.542	Carrier = −0.076, drug = 0.078
	N–O_A	−0.341	Carrier = −0.105, drug = 0.109
	N–H_A	−0.577	Carrier = −0.076, drug = 0.078

Site	System	Binding energy (eV)	Partial charge (e)	Final diameter (Å)
Al	Al–F_E	−3.842	Carrier = −0.655 Drug = 0.656	7.70
	Al–O_E	−3.006	Carrier = −0.571 Drug = 0.573	7.96
	Al–H_E	−3.691	Carrier = −0.602 Drug = 0.606	8.06
N	N–F_E	−3.357	Carrier = −0.616 Drug = 0.618	7.70
	N–O_E	−3.346	Carrier = −0.589 Drug = 0.589	8.44
	N–H_E	−3.346	Carrier = −0.648 Drug = 0.648	7.85

N–H_A, Al–O_A, and N–O_A displayed lower values. The pronounced charge transfer in Al–F_A arises from direct interactions between the electronegative fluorine atoms of 5-FU and the Lewis-acidic aluminum sites of the nanotube, allowing partial delocalization of lone pair electrons from fluorine to Al. In contrast, Al–O_A and N–O_A, interacting *via* oxygen, exhibited lower charge transfer ($\sim$0.260e and 0.214e, respectively), indicating weaker electronic coupling. These results highlight Al–F_A as the most electronically favorable surface-adsorbed system, suitable for rapid or burst-mode drug release.

Encapsulated systems displayed significantly higher charge transfer, typically exceeding 1.1e, due to enhanced molecular contact and stronger electrostatic and hydrogen-bonding interactions within the nanotube cavity. Al–F_E exhibited the highest charge redistribution, followed by Al–H_E and N–H_E, confirming its electronic stability and kinetic robustness. These findings demonstrate that encapsulation promotes stronger host–guest electronic coupling, supporting sustained drug retention and controlled release.[68]

3.6.3. Structural deformation. The mechanical response of the nanotube upon drug loading was evaluated by monitoring the diameter changes before and after interaction with 5-FU. Pristine-functionalized AlNNTs had a uniform diameter of 8.51 Å. Surface-adsorbed systems exhibited negligible changes, confirming that adsorption occurs *via* weak physisorption without imposing structural strain. This structural preservation is advantageous for rapid-release delivery, where mechanical integrity and reversibility are critical.

Encapsulated systems showed pronounced contraction, with diameters ranging from 8.44 Å to 7.70 Å. Al–F_E and N–F_E displayed the most significant shrinkage ($\sim$9.5%), reflecting strong steric and electrostatic confinement within the nanotube cavity. Intermediate reductions were observed in Al–H_E (8.06 Å), N–H_E (7.85 Å), and Al–O_E (7.96 Å), indicating effective encapsulation with slightly reduced molecular tension. These structural changes correlate with adsorption energies and Mulliken charge transfer, demonstrating that stronger electronic interactions are often accompanied by greater radial deformation.[69]

Collectively, these analyses highlight the contrasting behaviors of surface adsorption and encapsulation. A-series systems maintain geometric integrity, making them ideal for rapid or reversible delivery, with Al–F_A emerging as the most favourable surface-adsorbed configuration. In contrast, E-series systems exhibit significant confinement and structural adaptation, consistent with sustained or stimuli-responsive drug release, with Al–F_E representing the most structurally and electronically favorable encapsulated nanocarrier among the studied configurations.

3.7. Molecular dynamics simulations

To investigate the dynamic behavior and thermal stability of the drug–nanocarrier complexes under physiologically relevant conditions, Molecular Dynamics (MD) simulations were performed using the NPT ensemble as implemented in QuantumATK. The simulations were carried out for the two most stable configurations identified from prior DFT analyses, namely the surface-adsorbed (Al–F_A) and encapsulated (Al–F_E) systems (Fig. 8). Temperature regulation was achieved using a Berendsen thermostat with a target temperature of 300 K and a thermostat relaxation time of 10 ps, ensuring controlled thermal equilibration. Pressure was maintained at 1 bar using the Berendsen barostat, with a relaxation time of 1000 fs and a compressibility of 0.0001 bar^{-1}. Pressure coupling was applied isotropically along the diagonal components (xx, yy, zz). A time step of 1 fs was employed, and each system was propagated for 10 000 MD steps, corresponding to a total simulation duration of 10 ps. Initial atomic velocities were assigned according to the Maxwell–Boltzmann distribution at 300 K. To eliminate artificial translational motion, the center-of-mass momentum was removed at the beginning of the simulation. These simulation conditions ensured stable thermodynamic control and enabled reliable evaluation of the structural fluctuations, equilibration characteristics, and energetic stability of the drug–nanocarrier complexes.[67]

The total and potential energy trajectories confirmed that both surface-adsorbed and encapsulated systems reached thermodynamic equilibrium and remained dynamically stable throughout the simulation period. Energy profiles remained effectively constant, with no evidence of desorption, abrupt fluctuations, or drift, indicating that both drug–nanocarrier assemblies are thermomechanically robust under physiological thermal conditions and that the nanotube framework preserves structural integrity while retaining the drug molecule.

For the surface-adsorbed Al–F_A system, the potential energy fluctuated narrowly around –1033 eV, reflecting limited atomic rearrangement and a rigid interface. This behavior is consistent with non-covalent physisorption dominated by van der Waals and dipole–dipole interactions. The constrained conformational dynamics of 5-FU suggest a readily releasable

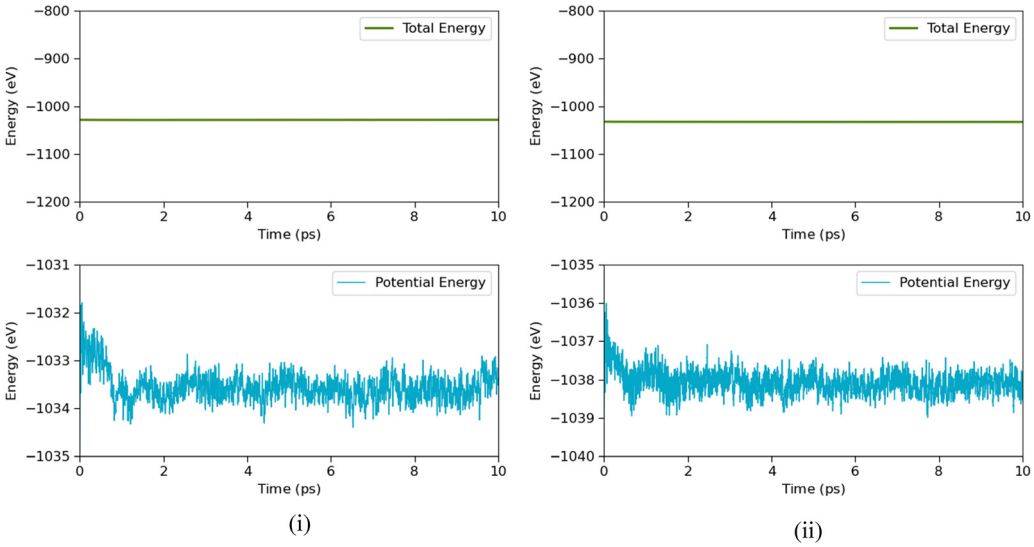

Fig. 8 MD simulations for (i) drug adsorption and (ii) drug encapsulation.

state, confirming the suitability of this configuration for burst-release or short-term therapeutic delivery. In contrast, the encapsulated Al–F_E system exhibited a deeper potential energy well, stabilizing near −1038 eV. Initial fluctuations during the first 2 ps correspond to the early-stage relaxation of 5-FU within the nanotube cavity, followed by a steady potential energy profile indicative of strong molecular confinement and effective host–guest interactions.[70] These dynamic behaviors are consistent with prior DFT-derived descriptors, including more negative adsorption and binding energies, significant Mulliken charge transfer, and structural adaptation, supporting the potential of Al–F_E for sustained-release, long-circulating, or stimuli-responsive drug delivery.

Overall, the MD simulations reinforce the complementary suitability of the two systems for distinct therapeutic strategies: Al–F_A (surface adsorption) for rapid, surface-mediated drug release and Al–F_E (encapsulation) for encapsulation-driven, long-term delivery. Both configurations demonstrate dynamic and thermomechanical robustness under biologically relevant conditions, highlighting their potential as reliable and adaptable nanocarriers.

3.8. Activation energy barrier for 5-FU desorption from the functionalized AlNNT

The desorption kinetics of 5-fluorouracil (5-FU) from [AlNNT(SA)2(C═O)] were investigated using the Nudged Elastic Band (NEB) method to determine the minimum energy pathways (MEPs) and corresponding activation energy barriers (E_a) between bound and unbound states. Two representative configurations were analyzed: (i) encapsulated 5-FU within the nanotube channel (Al–F_E) and (ii) surface-adsorbed 5-FU on the nanotube sidewall (Al–F_A) (Fig. 9). This approach provides a quantitative understanding of the thermally accessible release pathways and the kinetics governing drug detachment under physiologically relevant conditions.

For the encapsulated system, nine intermediate images revealed an energy profile featuring multiple local minima separated by moderate energy barriers. The maximum

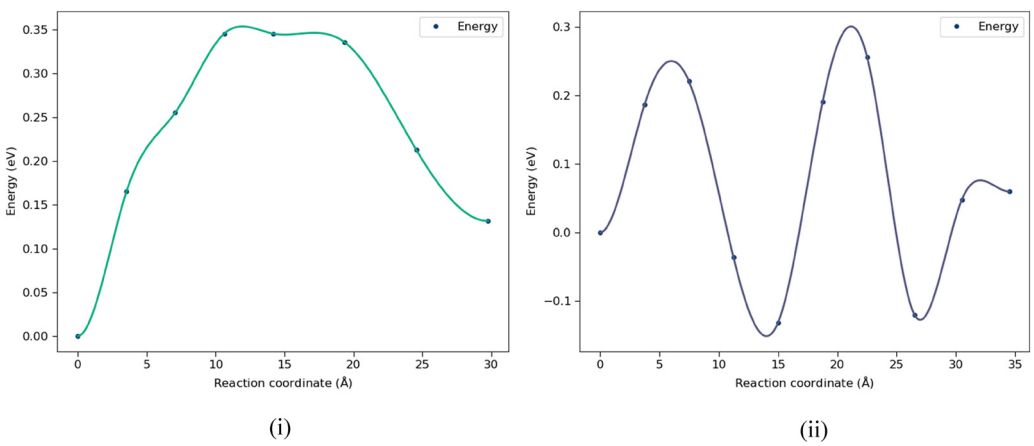

Fig. 9 NEB energy profiles for (i) drug adsorption and (ii) drug encapsulation systems.

activation energy along the pathway was calculated to be 0.187 eV. These metastable states arise from transient van der Waals interactions and hydrogen bonding with the functionalized inner wall, reflecting a stepwise desorption mechanism that stabilizes the drug within the nanotube cavity.[71] In contrast, the surface-adsorbed pathway, modeled with eight intermediate images, displayed a smoother energy profile with a single barrier of 0.165 eV, indicating a kinetically simpler detachment process consistent with non-covalent physisorption.

All NEB calculations were converged to a force tolerance of 0.05 eV $Å^{-1}$ for both standard and climbing images, using up to 2000 optimization steps to accurately resolve saddle points along the pathways. The barrier heights ($\sim$0.16–0.19 eV) are several times higher than the thermal energy at 300 K ($kT \approx$ 0.026 eV), suggesting that drug release can occur under physiological conditions while encapsulation provides stronger retention than surface adsorption.[72] These results align with previous DFT-derived descriptors, including more negative adsorption energies, substantial Mulliken charge transfer, and observed structural adaptation, collectively demonstrating that encapsulated 5-FU experiences tighter molecular confinement and stronger host–guest interactions.

Overall, the NEB analysis confirms that [AlNNT(SA)2(C═O)] with 5-FU achieves an optimal balance between drug stabilization and controlled release kinetics. Surface adsorption (Al–F_A) allows facile, rapid release suitable for burst delivery, whereas encapsulation (Al–F_E) ensures prolonged retention, sustained release, and stimuli-responsive behavior. These findings further validate the potential of functionalized AlNNTs as robust, tunable, one-dimensional nanocarriers for targeted chemotherapeutic delivery.

4. Conclusions

This study demonstrates that dual-side chemical functionalization provides an effective strategy for tailoring the drug-delivery behaviour of aluminum nitride nanotubes. The introduction of sorbic acid, butyric acid, amine, and carbonyl groups creates a controlled surface environment that regulates the interaction of 5-fluorouracil with the nanotube surface, leading to predictable retention and release characteristics. These results highlight that the therapeutic performance of one-dimensional nanomaterials can be directed through rational surface-chemistry design rather than structural modification alone. The broader significance of this work lies in establishing clear relationships between functional-group chemistry, interfacial polarity, and drug-binding behaviour. Such insights are highly relevant for improving the precision, stability, and safety of chemotherapeutic delivery platforms. The demonstrated ability to modulate molecular affinity using simple and biocompatible modifications positions functionalized AlNNTs as a promising basis for designing adaptable and high-performance nanocarriers for targeted cancer therapy. Future work will focus on extending this chemical-design framework to multi-drug loading systems and evaluating how pH-dependent interactions influence retention and release behaviour. These computational directions will support the development of versatile AlNNT-based platforms capable of meeting the evolving needs of precision anticancer treatment.

Author contributions

All authors of this manuscript contributed to this research study.

Conflicts of interest

The authors declare that they have no known competing financial interests or personal relationships that could have appeared to influence the work reported in this paper.

Data availability

Data will be made available by the corresponding author upon reasonable request. Supplementary information includes optimized structures, tabulated data, density of states (DOS), and electron density difference (EDD) analyses. See DOI: https://doi.org/10.1039/d5tb02632f.

Acknowledgements

The authors gratefully acknowledge the financial support for this work from the DST-FIST, Government of India (Ref. No. SR/FST/PSI-155/ 2010). The authors convey their special thanks to the High-Performance Computing Centre, SRMIST, for providing the computational facility.

References

1 S. Senapati, A. K. Mahanta, S. Kumar and P. Maiti, Controlled drug delivery vehicles for cancer treatment and their performance, *Signal Transduction Targeted Ther.*, 2018, **3**(1), 7, DOI: 10.1038/s41392-017-0004-3.
2 R. Safaiee, H. Aminzadeh, A. R. Sardarian, S. Nasresfahani and M. H. Sheikhi, A high loading nanocarrier for the 5-fluorouracil anticancer drug based on chloromethylated graphene, *Phys. Chem. Chem. Phys.*, 2024, **26**(7), 6410–6419, DOI: 10.1039/D3CP04211A.
3 A. Almomen and A. Alhowyan, A comprehensive study on Folate-Targeted mesoporous silica nanoparticles loaded with 5-Fluorouracil for the enhanced treatment of gynecological cancers, *J. Funct. Biomater.*, 2024, **15**(3), 74, DOI: 10.3390/jfb15030074.
4 P. M. Arvejeh, F. A. Chermahini, F. Marincola, F. Taheri, S. A. Mirzaei, A. Alizadeh, F. Deris, R. Jafari, N. Amiri, A. Soltani and E. Bijad, A novel approach for the co-delivery of 5-fluorouracil and everolimus for breast cancer combination therapy: stimuli-responsive chitosan hydrogel embedded with mesoporous silica nanoparticles, *J. Transl. Med.*, 2025, **23**(1), 382, DOI: 10.1186/s12967-025-06396-4.

5 X. Cong, Z. Zhang, H. Li, Y. G. Yang, Y. Zhang and T. Sun, Nanocarriers for targeted drug delivery in the vascular system: focus on endothelium, *J. Nanobiotechnol.*, 2024, **22**(1), 620, DOI: 10.1186/s12951-024-02892-9.
6 M. S. Kang, M. Kwon, H. J. Jang, S. J. Jeong, D. W. Han and K. S. Kim, Biosafety of inorganic nanomaterials for theranostic applications, *Emergent Mater.*, 2022, **5**(6), 1995–2029, DOI: 10.1007/s42247-022-00426-3.
7 S. Motta, P. Siani, A. Levy and C. Di Valentin, Exploring the drug loading mechanism of photoactive inorganic nanocarriers through molecular dynamics simulations, *Nanoscale*, 2021, **13**(30), 13000–13013, DOI: 10.1039/D1NR01972D.
8 R. O. Saleh, D. O. Bokov, M. N. Fenjan, W. K. Abdelbasset, U. S. Altimari, A. T. Jalil, L. Thangavelu, W. Suksatan and Y. Cao, Application of aluminum nitride nanotubes as a promising nanocarriers for anticancer drug 5-aminosalicylic acid in drug delivery system, *J. Mol. Liq.*, 2022, **352**, 118676, DOI: 10.1016/j.molliq.2022.118676.
9 N. Suleiman, V. Apalangya, K. Kan-Dapaah, B. Mensah, V. W. Elloh, A. Yaya and E. K. Abavare, Adsorption of CO and CO2 interaction with (7, 0) AlN nanotubes to enhance sensing capabilities: a DFT approach, *J. Phys. Chem. Solids*, 2025, **199**, 112537, DOI: 10.1016/j.jpcs.2024.112537.
10 M. Zhao, Y. Xia, D. Zhang and L. Mei, Stability and electronic structure of AlN nanotubes, *Phys. Rev. B: Condens. Matter Mater. Phys.*, 2003, **68**(23), 235415, DOI: 10.1103/PhysRevB.68.235415.
11 Z. Liu, W. Li, Z. Qin, L. Jin, Z. Sun and H. Wu, Research on the Stability of Different Polar Surfaces in Aluminum Nitride Single Crystals, *Crystals*, 2024, **14**(4), 337, DOI: 10.3390/cryst14040337.
12 N. Ahammad, A. U. Rahman, M. A. Kabir and M. K. Sikder, A Computational Investigation on the Structural, Thermodynamic, Electrical, Magnetic, and Optical Properties of Transition Metal (Cr & Mo)-Doped Aluminum Nitride Nanotubes Using Density Functional Theory, *Nano*, 2025, 2550073, DOI: 10.1142/S1793292025500730.
13 M. Adel, P. Keyhanvar, M. Zahmatkeshan, M. Bayandori, S. Teimourian, S. Hooshyar and N. Keyhanvar, Boron nitride nanotubes: Unlocking a new frontier in biomedicine, *Bionanoscience*, 2025, **15**(2), 226, DOI: 10.1007/s12668-025-01843-4.
14 A. Hassanpour, M. Zamanfar, S. Ebrahimiasl, A. Ebadi and P. Liu, Dopamine drug adsorption on the aluminum nitride single-wall nanotube: An ab initio study, *Arabian J. Sci. Eng.*, 2022, **47**(1), 477–484, DOI: 10.1007/s13369-021-05678-5.
15 P. Hassanpour, Y. Panahi, A. Ebrahimi-Kalan, A. Akbarzadeh, S. Davaran, A. N. Nasibova, R. Khalilov and T. Kavetskyy, Biomedical applications of aluminium oxide nanoparticles, *Micro Nano Lett.*, 2018, **13**(9), 1227–1231, DOI: 10.1049/mnl.2018.5070.
16 B. Makiabadi, M. Zakarianezhad and S. S. Hosseini, Investigation and comparison of pristine/doped BN, AlN, and CN nanotubes as drug delivery systems for the tegafur drug: A theoretical study, *Struct. Chem.*, 2021, **32**(3), 1019–1033, DOI: 10.1007/s11224-020-01680-z.
17 X. Gong, L. Guo and R. Zhou, Exploring the potential use of aluminium nitride nanoparticles in the delivery of flutamide anticancer drug, *Inorg. Chem. Commun.*, 2023, **158**, 111478, DOI: 10.1016/j.inoche.2023.111478.
18 X. Li, Aluminium nitride as an efficient catalyst in the synthesis of some chromeno [4, 3-b] chromenes and potential nanocarrier for delivery of flutamide, *Chem. Pap.*, 2024, **78**(2), 1157–1166, DOI: 10.1007/s11696-023-03154-y.
19 Q. Wu, Z. Hu, X. Wang, Y. Lu, X. Chen, H. Xu and Y. Chen, Synthesis and characterization of faceted hexagonal aluminum nitride nanotubes, *J. Am. Chem. Soc.*, 2003, **125**(34), 10176–10177.
20 A. Solhjoo, Z. Sobhani, A. Sufali, Z. Rezaei, S. Khabnadideh and A. Sakhteman, Exploring pH dependent delivery of 5-fluorouracil from functionalized multi-walled carbon nanotubes, *Colloids Surf., B*, 2021, **205**, 111823, DOI: 10.1016/j.colsurfb.2021.111823.
21 R. V. Kamble, S. D. Bhinge, S. K. Mohite, D. S. Randive and M. A. Bhutkar, In vitro targeting and selective killing of MCF-7 and COLO320DM cells by 5-fluorouracil anchored to carboxylated SWCNTs and MWCNTs, *J. Mater. Sci.: Mater. Med.*, 2021, **32**(6), 71, DOI: 10.1007/s10856-021-06540-8.
22 E. González-Lavado, L. Valdivia, A. García-Castaño, F. González, C. Pesquera, R. Valiente and M. L. Fanarraga, Multi-walled carbon nanotubes complement the antitumoral effect of 5-fluorouracil, *Oncotarget*, 2019, **10**(21), 2022, DOI: 10.18632/oncotarget.26770.
23 S. Bogadi, M. Bhaskaran, V. Ravichandran, J. Nesamony, S. Chelliah, G. Kuppusamy, G. M. Prakash, V. V. Karri, S. Mallick, F. Farahim and T. Ali, Functionalized nanoparticles: a promising approach for effective management of Alzheimer's disease, *Mol. Neurobiol.*, 2025, 1–20, DOI: 10.1007/s12035-025-04917-2.
24 Z. Lule and J. Kim, Surface modification of aluminum nitride to fabricate thermally conductive poly (butylene succinate) nanocomposite, *Polymers*, 2019, **11**(1), 148, DOI: 10.3390/polym11010148.
25 P. Zhang, Q. Jiang and J. Li, Comparative study of silica nanoparticles and surface modified silica nanoparticles: Drug adsorption process and controlled release behavior, *Mater. Sci. Eng. B*, 2020, **259**, 114609, DOI: 10.1016/j.mseb.2020.114609.
26 C. Ferrand, F. Marc, P. Fritsch and G. de Saint-Blanquat, Sorbic acid-amine function interactions, *Food Addit. Contam.*, 1998, **15**(4), 487–493, DOI: 10.1080/02652039809374670.
27 B. Shashni and Y. Nagasaki, Short-chain fatty acid-releasing nano-prodrugs for attenuating growth and metastasis of melanoma, *Acta Biomater.*, 2023, **159**, 226–236, DOI: 10.1016/j.actbio.2023.01.054.
28 S. I. Marchesan and M. A. Prato, Under the lens: carbon nanotube and protein interaction at the nanoscale, *Chem. Commun.*, 2015, **51**(21), 4347–4359, DOI: 10.1039/c4cc09173f.
29 C. Y. Hsu, A. Yadav, S. M. Mohealdeen, Y. A. Abdulsayed, A. H. Adhab, S. Sharma, S. Aslanzadeh and B. Darabinajand,

Computational quantum mechanical investigation of the functionalized AlN nanotube as the smart carriers for levodopa drug delivery: a DFT analysis, *Bull. Mater. Sci.*, 2023, **47**(1), 10, DOI: 10.1007/s12034-023-03079-y.

30 A. Bizaval, Z. Karami Horastani and S. J. Hashemifar, DFT study of (6, 0) boron nitride nanotube as a drug delivery system for 5-fluorouracil and hydroxyurea, *Eur. Phys. J. Plus*, 2025, **140**(5), 356, DOI: 10.1140/epjp/s13360-025-06296-y.

31 Z. Ghavi, A. Torrik, M. Rezaee and M. Zarif, Molecular dynamics insights into non-covalent functionalization of boron nitride nanotubes for doxorubicin delivery, *Sci. Rep.*, 2025, **15**(1), 30213, DOI: 10.1038/s41598-025-15150-1.

32 L. Zhang, C. Wang, Y. Jiang, S. Zhang, D. Ye and L. Liu, Drug delivery mechanism of doxorubicin and camptothecin on single-walled carbon nanotubes by DFT study, *Appl. Surf. Sci.*, 2023, **614**, 156242, DOI: 10.1016/j.apsusc.2022.156242.

33 S. A. Al-Zuhairy, M. M. Kadhim, M. H. Shadhar, N. A. Jaber, H. A. Almashhadani, A. M. Rheima, M. N. Mousa and Y. Cao, Study to molecular insight into the role of aluminum nitride nanotubes on the delivery of 5-fluorouracil (5FU) drug in smart drug delivery, *Inorg. Chem. Commun.*, 2022, **142**, 109617, DOI: 10.1016/j.inoche.2022.109617.

34 C. Gan and P. Liu, Adsorption behavior of anticancer drug on the aluminum nitride surface: Density functional theory evaluation, *Phosphorus, Sulfur Silicon Relat. Elem.*, 2021, **196**(12), 1061–1070, DOI: 10.1080/10426507.2021.1966428.

35 V. Abinaya, K. J. Sivasankar, J. Sneha and D. J. Thiruvadigal, Organic acid-functionalized Aluminum Nitride Nanotubes (AlNNT) for targeted drug delivery using Carmustine: A DFT study, *Surf. Interfaces*, 2025, **64**, 106438, DOI: 10.1016/j.surfin.2025.106438.

36 S. Smidstrup, T. Markussen, P. Vancraeyveld, J. Wellendorff, J. Schneider, T. Gunst, B. Verstichel, D. Stradi, P. A. Khomyakov, U. G. Vej-Hansen and M. E. Lee, QuantumATK: an integrated platform of electronic and atomic-scale modelling tools, *J. Phys.: Condens. Matter*, 2019, **32**(1), 015901, DOI: 10.1088/1361-648X/ab4007.

37 N. A. Sakharova, A. F. Pereira, J. M. Antunes, B. M. Chaparro, T. G. Parreira and J. V. Fernandes, On the determination of elastic properties of single-walled nitride nanotubes using numerical simulation, *Materials*, 2024, **17**(10), 2444, DOI: 10.3390/ma17102444.

38 K. B. Thasan, C. Poornimadevi and D. J. Thiruvadigal, A First-Principles investigation on substitutionally doped & co-doped Boron Phosphide (BP) monolayer for hydrogen-based gas sensing, *Comput. Condensed Matter.*, 2025, e01091, DOI: 10.1016/j.cocom.2025.e01091.

39 P. Yan, A. A. Casale and J. W. Bennett, Modeling 2D van der Waals Materials with Homonuclear Bonds of Main Group Cations, *ACS Org. Inorg. Au*, 2026, **6**(1), 104–118, DOI: 10.1021/acsorginorgau.5c00096.

40 A. S. Gomes, K. G. Dyall and L. Visscher, Relativistic double-zeta, triple-zeta, and quadruple-zeta basis sets for the lanthanides La–Lu, *Theor. Chem. Acc.*, 2010, **127**(4), 369–381, DOI: 10.1007/s00214-009-0725-7.

41 V. Abinaya, D. J. Thiruvadigal, R. Akash, A. S. Balaji, R. M. Hariharan, J. Sneha, U. Adharsh and K. J. Sivasankar, Chemical modification of Aluminum Nitride Nanotubes (AlNNT) using-OH, C= O, R-SH functional groups: first principle's study, *Surf. Interfaces*, 2023, **41**, 103262, DOI: 10.1016/j.surfin.2023.103262.

42 M. Amin, M. M. Rahman, M. K. Rokunuzzaman, M. K. Hossain and F. Ahmed, First-principles study of aromatic amino acid encapsulation in single-walled BN and AlN nanotubes, *Comput. Theor. Chem.*, 2024, **1242**, 114954, DOI: 10.1016/j.comptc.2024.114954.

43 M. Rezaei-Sameti and P. N. Zarei, NBO, AIM, HOMO–LUMO and thermodynamic investigation of the nitrate ion adsorption on the surface of pristine, Al and Ga doped BNNTs: A DFT study, *Adsorption*, 2018, **24**(8), 757–767, DOI: 10.1007/s10450-018-9977-7.

44 M. Ghafari, H. Mohammadi-Manesh and F. K. Fotooh, Adsorption of formamide on pure, Al-, N-doped, and Al/N co-doped (8, 0) single-wall carbon nanotubes: a DFT study, *Eur. Phys. J. B*, 2024, **97**(4), 38, DOI: 10.1140/epjb/s10051-024-00679-3.

45 H. Shao, Y. Wang, J. Song, L. Lei, X. Liu, X. Hou and J. Zhang, First-Principles Calculation of Mechanical Properties and Thermal Conductivity of C-Doped AlN, *Ceramics*, 2025, **8**(3), 117, DOI: 10.3390/ceramics8030117.

46 M. T. Baei, A. A. Peyghan and Z. Bagheri, Covalent functionalization of AlN nanotubes with acetylene, *Phys. E*, 2013, **47**, 147–151, DOI: 10.1016/j.physe.2012.10.03.

47 J. Sneha, V. Abinaya, R. Akash, R. M. Hariharan, K. J. Sivasankar and D. J. Thiruvadigal, Exploring the structural and electronic properties of boron nitride nanotube (BNNT) as nanocarrier for drug delivery applications: DFT approach, *J. Comput.-Aided Mol. Des.*, 2025, **39**(1), 1–22, DOI: 10.1007/s10822-025-00641-0.

48 J. Sneha, K. J. Sivasankar, V. Abinaya and D. J. Thiruvadigal, A DFT Investigation on Functionalized Boron Nitride Nanotubes with Non-Essential Amino Acids for Targeted Cancer Drug Delivery of Allicin, *ChemistrySelect*, 2025, **10**(27), e01126, DOI: 10.1002/slct.202501126.

49 H. J. Shin, S. M. Kim, S. M. Yoon, A. Benayad, K. K. Kim, S. J. Kim, H. K. Park, J. Y. Choi and Y. H. Lee, Tailoring electronic structures of carbon nanotubes by solvent with electron-donating and-withdrawing groups, *J. Am. Chem. Soc.*, 2008, **130**(6), 2062–2066, DOI: 10.1021/ja710036e.

50 K. Z. Milowska and J. A. Majewski, Functionalization of carbon nanotubes with–CHn,–NHn fragments,–COOH and–OH groups, *J. Chem. Phys.*, 2013, **138**(19), 194704, DOI: 10.1063/1.4804652.

51 V. V. Shunaev, N. G. Bobenko, P. M. Korusenko, V. E. Egorushkin and O. E. Glukhova, Carboxyl functionalization of N-MWCNTs with Stone–Wales defects and possibility of HIF-1α wave-diffusive delivery, *Int. J. Mol. Sci.*, 2023, **24**(2), 1296, DOI: 10.3390/ijms24021296.

52 M. Rezazade, S. Ketabi and M. Qomi, Effect of functionalization on the adsorption performance of carbon nanotube as a drug delivery system for imatinib: molecular simulation

study, *BMC Chem.*, 2024, **18**(1), 85, DOI: 10.1186/s13065-024-01197-0.

53 O. I. Martin, M. A. Abed and K. Pathmanathan, A theoretical investigation into the adsorption of antimalarial drug pollutants on aluminum nitride nanotubes, *Diamond Relat. Mater.*, 2025, 112878, DOI: 10.1016/j.diamond.2025.112878.

54 J. Sneha, V. Abinaya, K. J. Sivasankar and D. J. Thiruvadigal, Computational insights into amino acid functionalized boron nitride nanotube (BNNT) as a tunable nanocarrier for drug delivery applications, *Results Surf. Interfaces*, 2025, 100648, DOI: 10.1016/j.rsurfi.2025.100648.

55 T. A. Baghemiyani and F. Kalantari Fotooh, Interaction of lead metal with single walled AlN nanotube: a computational study, *J. Inorg. Organomet. Polym. Mater.*, 2017, **27**(5), 1274–1280, DOI: 10.1007/s10904-017-0578-9.

56 Y. S. Itas, N. H. Alotaibi, S. Mohammad, R. Haldhar, S. C. Kim and M. K. Hossain, DFT studies on structural, electronic and optical properties of aluminum nitride nanotube doped by different concentrations of boron, *Mater. Chem. Phys.*, 2024, **320**, 129429, DOI: 10.1016/j.matchemphys.2024.129429.

57 J. Sneha, R. M. Hariharan, R. Akash, A. S. Balaji, D. J. Thiruvadigal, U. Adharsh, V. Abinaya and K. J. Sivasankar, Covalent modification of single-walled boron nitride nanotube (BNNT) with amino acids: Ab initio method, *Surf. Interfaces*, 2023, **42**, 103337, DOI: 10.1016/j.surfin.2023.103337.

58 F. N. Ajeel, K. H. Bardan, S. H. Kareem and A. M. Khudhair, Pd doped carbon nanotubes as a drug carrier for Gemcitabine anticancer drug: DFT studies, *Chem. Phys. Imp.*, 2023, **7**, 100298, DOI: 10.1016/j.chphi.2023.100298.

59 V. Abinaya, J. Sneha, R. Akash, R. M. Hariharan, K. J. Sivasankar and D. J. Thiruvadigal, Functionalization of single-walled aluminum nitride nanotube with amino acids using the first principle's study, *Surf. Interfaces*, 2024, **54**, 105216, DOI: 10.1016/j.surfin.2024.105216.

60 V. Abinaya, J. Sneha, K. J. Sivasankar and D. J. Thiruvadigal, Computational approach to drug delivery using fumaric acid functionalized AlNNT's as nanocarriers for hydroxyurea, *Results Surf. Interfaces*, 2025, 100708, DOI: 10.1016/j.rsurfi.2025.100708.

61 A. U. Rahman, D. M. Saaduzzaman, S. M. Hasan, M. Amin and M. K. Sikder, Aluminum-derived nanotubes for lung cancer detection: a DFT inquisition, *Sci. Rep.*, 2025, **15**(1), 34852, DOI: 10.1038/s41598-025-89999-7.

62 Z. Mahdavifar, N. Abbasi and E. Shakerzadeh, A comparative theoretical study of CO2 sensing using inorganic AlN, BN and SiC single walled nanotubes, *Sens. Actuators, B*, 2013, **185**, 512–522, DOI: 10.1016/j.snb.2013.05.004.

63 M. M. Kadhim, A. M. Rheima, S. K. Hachim, S. A. Abdullaha, T. Z. Taban and S. A. Malik, Theoretical sensing performance for detection of cyclophosphamide drug by using aluminum carbide (C3Al) monolayer: a DFT Study, *Appl. Biochem. Biotechnol.*, 2023, **195**(7), 4164–4176, DOI: 10.1007/s12010-022-04305-9.

64 W. Bououden, Y. Benguerba, A. S. Darwish, A. Attoui, T. Lemaoui, M. Balsamo, A. Erto and I. M. Alnashef, Surface adsorption of Crizotinib on carbon and boron nitride nanotubes as Anti-Cancer drug Carriers: COSMO-RS and DFT molecular insights, *J. Mol. Liq.*, 2021, **338**, 116666, DOI: 10.1016/j.molliq.2021.116666.

65 J. K. Patra, G. Das, L. F. Fraceto, E. V. Campos, M. D. Rodriguez-Torres, L. S. Acosta-Torres, L. A. Diaz-Torres, R. Grillo, M. K. Swamy, S. Sharma and S. Habtemariam, Nano based drug delivery systems: recent developments and future prospects, *J. Nanobiotechnol.*, 2018, **16**(1), 71, DOI: 10.1186/s12951-018-0392-8.

66 A. Soltani, M. T. Baei, E. T. Lemeski, S. Kaveh and H. Balakheyli, A DFT study of 5-fluorouracil adsorption on the pure and doped BN nanotubes, *J. Phys. Chem. Solids*, 2015, **86**, 57–64, DOI: 10.1016/j.jpcs.2015.06.008.

67 M. Zarghami Dehaghani, F. Yousefi, S. M. Sajadi, M. Tajammal Munir, O. Abida, S. Habibzadeh, A. H. Mashhadzadeh, N. Rabiee, E. Mostafavi and M. R. Saeb, Theoretical encapsulation of fluorouracil (5-FU) anti-cancer chemotherapy drug into carbon nanotubes (CNT) and boron nitride nanotubes (BNNT, *Molecules*, 2021, **26**(16), 4920, DOI: 10.3390/molecules26164920.

68 G. J. Ogunwale, H. Louis, T. O. Unimuke, G. E. Mathias, A. E. Owen, H. O. Edet, O. C. Enudi, E. O. Oluwasanmi, A. S. Adeyinka and M. Doust Mohammadi, Interaction of 5-fluorouracil on the surfaces of pristine and functionalized Ca12O12 nanocages: An intuition from DFT, *ACS Omega*, 2023, **8**(15), 13551–13568, DOI: 10.1021/acsomega.2c03635.

69 J. Streit, C. R. Snyder, J. Campo, M. Zheng, J. R. Simpson, A. R. Hight Walker and J. A. Fagan, Alkane encapsulation induces strain in small-diameter single-wall carbon nanotubes, *J. Phys. Chem. C*, 2018, **122**(21), 11577–11585, DOI: 10.1021/acs.jpcc.8b03166.

70 A. Faizi, Z. Kalantar and S. M. Hashemianzadeh, Drug delivery by SiC nanotubes as nanocarriers for anti-cancer drugs: investigation of drug encapsulation and system stability using molecular dynamics simulation, *Mater. Res. Express*, 2021, **8**(10), 105012, DOI: 10.1088/2053-1591/ac3107.

71 A. W. Ruttinger, D. Sharma and P. Clancy, Protocol for directing nudged elastic band calculations to the minimum energy pathway: Nurturing errant calculations back to convergence, *J. Chem. Theory Comput.*, 2022, **18**(5), 2993–3005, DOI: 10.1021/acs.jctc.1c00926.

72 G. Henkelman, B. P. Uberuaga and H. Jónsson, A climbing image nudged elastic band method for finding saddle points and minimum energy paths, *J. Chem. Phys.*, 2000, **113**(22), 9901–9904, DOI: 10.1063/1.1329672.